

Discerning the interactions between environmental parameters reflected in $\delta^{13}\text{C}$ and $\delta^{18}\text{O}$ of recent fluvial tufas: lessons from a Mediterranean climate region

M. Cinta Osácar^a, Concha Arenas^a, Luis Auqué^a, Carlos Sancho^a, Gonzalo Pardo^a,
Marta Vázquez-Urbez^a

a Departamento de Ciencias de la Tierra, Universidad de Zaragoza, C/Pedro Cerbuna
12, 50009 Zaragoza, Spain

cinta@unizar.es, carenas@unizar.es, lauque@unizar.es, csancho@unizar.es,
gpardo@unizar.es, m.vazquez.urbez@gmail.com

Abstract

$\delta^{13}\text{C}$ and $\delta^{18}\text{O}$ of recent, continuous tufa records, obtained during a monitoring period spanning 3 to 13 years, are compared with the corresponding, known environmental conditions. Three rivers in NE Iberia (located along a 200-km N-S transect) are used for this comparison. The isotopic variations through space and time are discussed in terms of the environmental and geological parameters that operate on different scales, focusing on discerning the interactions between these parameters and providing examples of possible misinterpretation of climatic conditions, which is important to past climate studies based on isotopic data.

The calculation of the actual isotopic fractionation coefficients, and the comparison with the literature-derived coefficients, demonstrates that the studied tufa formation was close to isotopic equilibrium to reflect the water temperature. The difference between mean measured water temperature (T_w) and mean calculated T_w (based on $\delta^{18}\text{O}_{\text{calcite}}$ and measured $\delta^{18}\text{O}_{\text{water}}$) is less than 2.7°C. Tendencies of these calculated T_w are similar to the regional air temperature (T_{air}) tendencies through time, in particular in the case of the 13-year record, although certain deviations exist over shorter time spans. The best

agreement between measured and calculated Tw and between $\delta^{18}\text{O}_{\text{calcite}}$ -based Tw tendencies and Tair tendencies corresponds to the tufa stromatolite facies.

Differences between the $\delta^{18}\text{O}_{\text{calcite}}$ records of the three rivers cannot be attributed to temperature changes, but to the varying influences of groundwater inputs and isotopic rainfall composition in each river. Without considering these parameters, $\delta^{18}\text{O}_{\text{calcite}}$ -based Tw calculations yield inaccurate results when comparing the study sites.

$\delta^{13}\text{C}_{\text{calcite}}$ values do not exhibit distinct patterns over time, and $\delta^{13}\text{C}_{\text{calcite}}$ variations are likely caused by local processes that do not reflect general environmental changes.

These findings underscore the significance of accounting for both groundwater behaviour and rainfall stable isotope composition when interpreting climate parameters in carbonate systems, particularly when differences between the isotopic signatures of deposits exist in the same region.

Keywords: Fluvial tufa, stable isotopes, periodic monitoring, seasonal changes, temperature tendencies, regional climatic variations

1 Introduction

Fluvial tufa deposits have been widely used as paleoenvironmental tools (e.g., as summarized by Pedley, 2009 and Capezzuoli et al., 2014), especially the stable isotopic composition of tufa calcite, due to the temperature dependence of the oxygen isotopic fractionation and the influence of several inorganic and organic carbon sources on carbon isotopes (Andrews, 2006). Obtaining reliable environmental information from stable isotopes is dependent upon calcite precipitation occurring in isotopic equilibrium. In some cases, the isotopic equilibrium was sufficient enough to provide trustworthy information (Matsuoka et al., 2001; Garnett et al., 2004; Kano et al., 2007; Yan et al.,

2012; Osácar et al., 2013a), while other studies have concluded that tufa precipitated at non equilibrium (Lojen et al., 2009; Yan et al., 2012; Sun et al., 2014). These results show the varied isotopic behaviours of fluvial systems.

In addition to above-mentioned parameters, other factors such as rainfall amount, moisture sources (Liu et al., 2006; Liu et al., 2010), residence time of water in an aquifer, discharge and other hydrological features (Wang et al., 2014) can produce varying effects on the tufa isotopic composition. These factors can be assessed based on the tufa isotopic record (Makhnach et al., 2004; Garnett et al., 2004). Together, these facts illustrate the complexity of the relationships between tufa stable isotopes and environmental conditions.

One of the most successful approaches for better understanding the tufa formation is the study of modern tufa sedimentation through periodic monitoring of both tufa stable isotopes and the related environmental parameters, such as physical and chemical water characteristics, air temperature and precipitation (Chafetz et al., 1991; Liu et al. 1995; Matsuoka et al. 2001; Kano et al. 2004; Lojen et al. 2004; O'Brien et al. 2006; Anzalone et al. 2007; Arenas et al. 2010; Brasier et al., 2010; Vázquez et al. 2010; Manzo et al. 2012; Yan et al., 2012; Osácar et al., 2013a; Auqué et al., 2014; Sun et al., 2014; Wang et al., 2014; Arenas et al., 2015).

Studies of modern tufa sedimentation in several rivers in the Iberian Range were conducted from 1999 to 2012 (Arenas et al. 2010; Vázquez-Urbez et al. 2010, 2011; Osácar et al., 2013a, b; Auqué et al., 2013, 2014; Arenas et al. 2014; Arenas et al., 2015), revealing that the Añamaza, Piedra and Ebrón Rivers (Fig. 1) are suitable for analysing the environmental imprint on the $\delta^{13}\text{C}$ and $\delta^{18}\text{O}$ records. These rivers, which are located along an approximately 200-km N-S transect in the Iberian Range (Fig. 1), share similar geologic contexts and climatic conditions, with a $\text{HCO}_3\text{-Ca-SO}_4$ -based

groundwater supply. Mechanical CO₂ outgassing is the primary driving mechanism of calcite precipitation in the three rivers. However, every river has unique features derived from specific conditions (discharge, precipitation, temperature, hydrodynamics and riverbed slope), which prompts the study of their effects on the isotopic composition of tufa sediment. Previous studies in these rivers (Osácar et al 2013a; Auqué et al., 2014; Arenas et al., 2014, 2015), dealt with the isotopic composition of tufa sediment sampled in situ twice a year, which represented short time spans and therefore, were a non-continuous record through time; moreover, these works focused greatly on the precipitation process in each river.

The main objective of this paper is to assess how diverse environmental parameters and factors are reflected in the tufa isotopic record and to determine the effects of their variations through space and time. For this purpose, continuous carbonate records, obtained from artificial substrates in three rivers in the Iberian Range and that are representative of the whole studied time period, are compared, and their stable isotope variations through space and time are discussed in terms of the involved environmental parameters. The results are of high interest to climatic interpretations based on stable isotopic data of the geological record.

2 Study Sites

2.1 Geographical, geological and climatic settings

The three study sites are located along a 200-km N-S transect in the Iberian Ranges (Fig. 1). The Añamaza and Piedra Rivers flow towards the NE into the Ebro River, and the Ebrón River flows to the SE into the Turia River. The Iberian Ranges are NW–SE trending, alpine, intraplate mountain chains on the northeastern Iberian Peninsula (Fig. 1). Thick Mesozoic carbonate formations are widespread and constitute karstic aquifers

that feed the entrenched drainage network (Table A1). The three studied rivers are mainly fed by groundwater. Karstic system dynamics produced extensive fluvial tufa sequences during the Quaternary (Peña et al., 2014; Sancho et al., 2015), and tufa formation remains active today in many valleys, including at the sites analysed in this study.

The climate in the region is continental Mediterranean with strong seasonal contrasts in temperature and precipitation. Precipitation is irregularly distributed with maxima in spring and autumn. The Atlantic rainfall fronts cross the Iberian Peninsula from west to east, with greater influence in the north. The eastern part of the peninsula is influenced by Mediterranean air masses (Araguás-Araguás and Díaz-Teijeiro, 2005). Table A1 summarizes geological and climatic information in the three river watersheds.

2.2 Sedimentological characteristics of the fluvial tufa systems

Carbonate sedimentation in the three studied rivers occurred in different depositional settings (subenvironments) defined by the morphological features of the riverbed (e.g., bed slope), physical flow characteristics (e.g., water velocity and depth) and substrate-associated biota (e.g., floral associations and bacteria). The distinct sedimentary carbonate facies that formed in the five main stream subenvironments are described in Arenas et al. (2014).

The deposits that formed in these subenvironments had very different deposition rates (mean values of facies from the three rivers varied from 0.1 to 12.8 mm/year), mainly linked to varying hydrodynamics. Mechanical CO₂ outgassing is considered the principal factor that controls tufa sedimentation (Arenas et al., 2014, Auqué et al., 2014, Arenas et al., 2015), as it occurs in other tufa systems (Chen et al. 2004; Gradzinski et al., 2010). Moreover, the locations of spring water inputs and the topographic profile of

the riverbed also determine the amount of CO₂ in water and, hence, the calcite saturation index variation along the rivers.

The deposition rates were greater during warm periods (spring and summer seasons) than during cool periods (autumn and winter seasons), independent of facies. These differences were mainly caused by seasonal variations in temperature-dependent parameters, such as water saturation with respect to calcite, the development of flora and prokaryotes and the correlative photosynthetic activity. Thus, tufa deposition rates in the studied rivers were controlled by both physicochemical and biological processes (Arenas et al., 2014; Auqué et al., 2014, Arenas et al., 2015).

The tufa records studied in this work correspond to two facies (Arenas et al, 2014):

- 1) Facies A is composed of stromatolites that formed in areas of fast flowing water (water velocity > 90 cm/s), such as rapids and small waterfalls devoid of mosses and filamentous algae (Fig. 2A). The laminated deposits (micrometre- to millimetre-thick laminae, Fig. 2B) consist of calcite tube-shaped bodies that formed around filamentous cyanobacteria that later decayed (Fig. 2C). The mean deposition rate was 12.8 mm/yr.
- 2) Facies C is composed of moss and algal boundstones that formed in stepped waterfalls and small waterfalls in slow to fast flowing water (Fig. 2D, E) in which mosses and filamentous algae were coated by calcite (Fig. 2F). The mean deposition rate was 6.8 mm/yr. Stromatolites (facies A) also formed in this subenvironment in zones with strong water flow (Fig. 2E, F).

2.3 Hydrochemistry

Waters of the Piedra and Ebrón rivers are HCO₃-Ca type at the headwaters, shifting towards a HCO₃-(SO₄)-Ca type downstream. Those of the Añamaza River are SO₄-HCO₃-Ca type (Auqué et al. 2014; Arenas et al., 2015). This characteristic explains the

high conductivity values found in the Añamaza River, as well as the higher dissolved SO_4 and Ca contents with respect to the two other rivers (Table A1). Mean pH (approximately 7.95 for the three rivers) and alkalinity values were very similar in the three rivers (Table A1).

The calculated partial pressure of CO_2 (pCO_2) was highest at the headwaters and decreased downstream due to CO_2 outgassing, especially at topographic breaks (Table A1). This general trend can be altered by additional groundwater inputs along the studied stretches, promoting local increases in pCO_2 values. The river waters were in equilibrium or oversaturated with respect to calcite (see the maximum saturation index (SIc) in Table A1).

The downstream evolution of Ca content and alkalinity suggests that tufa formation is a continuous process year round and is more intense in warm periods, which is in agreement with thickness measured in tablets (Arenas et al., 2014, 2015; Auqué et al. 2014).

3 Methods

Tufa analysed in this work was collected from sediment deposited on artificial substrates (limestone tablets 25x16x2 cm) that had been installed at sites that corresponded to different subenvironments along the three studied rivers (Fig. 1 and Fig. 2). One tablet was installed at each site. Ten sites along the Añamaza River were monitored from April 2007 to March 2010, nine sites along the Ebrón River were monitored from November 2006 to March 2010 and 24 sites along the Piedra River were monitored from November 1999 to September 2012. The tablets were removed at the end of summer and at the end of winter to measure the sediment thickness and then placed back in their original positions until the next six-month period ended. The

difference in sediment height between consecutive measuring times represented the six-month deposition rate at each site (see procedure in Vázquez-Urbez et al., 2010). In the Piedra River, up to four sets of tablets per site were installed throughout the entire monitoring period (Arenas et al. 2014). Spring and summer months are considered the warm period, while autumn and winter months represent the cool period. Hereafter, these periods are referred to as Warm and Cool. After the tablets were finally removed, they were cut perpendicularly to the accumulation surface. The six-month intervals were identified in the cross-sections by plotting the successive thickness measurements corresponding to the cut section.

Only tablets with relatively continuous sedimentary records (facies A and C) and in which six-month intervals could be clearly identified were selected for this study, including tablets from two sites in the Añamaza River, eight sites in the Piedra River (in the Monasterio de Piedra Park) and two sites in the Ebrón River (Fig. 1, 2 and Table 1). Samples for stable isotope analyses were collected with a microdrill. One sample per interval was taken, and within some intervals, up to three samples were obtained from base to top. Both facies A and C were sampled in some intervals.

Tufa consisted of calcite, as determined by X-ray diffraction analysis (see procedure in Osácar et al., 2013a). Textural observations of the deposits on tablets were made using a stereomicroscope and scanning electron microscopy (JEOL JSM 6400 at the University of Zaragoza). Thin sections of deposits on tablets were also examined using a petrographic microscope.

River water was sampled for chemical and $\delta^{18}\text{O}$ analysis every six months, in the middle of the warm periods (end of June) and cool periods (beginning of January), at a number of sites coinciding with the tablet sites (Fig. 1). Temperature, pH and conductivity were measured on site. Water temperature (T_w), which was obtained

hourly using data loggers (HOBO Pro V2; Onset, Cape Cod, Massachusetts, USA) installed in every river from June 2007 onwards, was also used in this work. Hereafter, we refer to the continuous Tw record unless otherwise stated. The water sampling procedure used in and the hydrochemical data from the Añamaza, Piedra and Ebrón rivers are detailed in Auqué et al. (2014) and Arenas et al. (2014, 2015).

$\delta^{13}\text{C}$ and $\delta^{18}\text{O}$ analyses of calcite ($\delta^{13}\text{C}_{\text{calcite}}$ and $\delta^{18}\text{O}_{\text{calcite}}$) and $\delta^{18}\text{O}$ analyses of water ($\delta^{18}\text{O}_{\text{water}}$) were performed at the Stable Isotope Analysis Service of the University of Salamanca (Spain). The analytical protocols and methods are outlined in Osácar et al. (2013a). The results are reported in $\delta\%$ notation relative to V-PDB (carbonates) and V-SMOW (water). The overall reproducibility was greater than $\pm 0.1\%$. A total of 181 calcite samples were analysed (85 from cool periods and 96 from warm periods, see Table 2, A2). Water $\delta^{18}\text{O}$ data from the three rivers (220 samples, Tables 1 and A2) were taken from Auqué et al., (2014), Osácar et al. (2013a) and Arenas et al. (2015).

Analyses of dissolved inorganic carbon in water ($\delta^{13}\text{C}_{\text{DIC}}$) in the Añamaza and Ebrón Rivers were carried out in the Cool 2009-2010 and Warm 2010 periods (Tables 1 and A2). $\delta^{13}\text{C}_{\text{DIC}}$ analyses were performed at the Department of Environmental Sciences of the J. Stefan Institute in Ljubljana (Slovenia) using the protocols described in Osácar et al. (2013a). The results are expressed in $\delta\%$ notation and are reported versus V-PDB. Reproducibility was greater than $\pm 0.1\%$. $\delta^{13}\text{C}_{\text{DIC}}$ data from the Piedra River were taken from Osácar et al. (2013a) from the Cool 2009-2010 to Warm 2012 periods (Tables 1 and A2).

The water temperature was calculated using the formula reported by O'Brien et al. (2006), which was applied to similar tufa sediments (Osácar et al., 2013a):

$$T(^{\circ}\text{C})=15.310-4.478(\delta^{18}\text{O}_{\text{calcite}}-\delta^{18}\text{O}_{\text{water}})+0.14[0.277+1.0412(\delta^{18}\text{O}_{\text{calcite}}-\delta^{18}\text{O}_{\text{water}})]^2(1)$$

$\delta^{18}\text{O}_{\text{water}}$ values of precipitation of several stations close to the rivers (Soria, year 2003, Madrid-Retiro, Zaragoza and Valencia, years 2000 to 2009 in the three cases) were taken from the Spanish Stations of the Red de Vigilancia de Isótopos en la Precipitación (REVIP, the Spanish member of the Global Network of Isotopes in Precipitation, GNIP) and compared with the river $\delta^{18}\text{O}_{\text{water}}$ values.

4 Results

4.1 Water temperature (T_w)

The lowest average T_w corresponds to the Añamaza River, both in cool and warm periods, while the highest average T_w corresponds to the Ebrón River in cool periods and to the Piedra River in warm periods (Table 1). The Piedra River exhibits the widest T_w range (even based on only the synchronous time interval). The narrowest T_w range corresponds to the Ebrón River (Fig. A1).

4.2 Water $\delta^{13}\text{C}$ and $\delta^{18}\text{O}$ composition

Mean $\delta^{13}\text{C}_{\text{DIC}}$ values (Fig. A2A) are significantly lower in January than in June in the Añamaza and Ebrón rivers, but in the Piedra River, the June and January values are similar (Table 1). In the Piedra River the $\delta^{13}\text{C}_{\text{DIC}}$ values at different sites are within a narrower range (Table A2), and the average $\delta^{13}\text{C}_{\text{DIC}}$ value becomes progressively higher from Cool 2009-2010 to Warm 2012 (Fig. 3). The $\delta^{13}\text{C}_{\text{DIC}}$ values of the River Piedra spring (-11.3 and -11.4‰V-PDB in January and June 2010, respectively) are notably lower than those of the Añamaza and Ebrón rivers (-10.6‰ and -9.6‰V-PDB in January and June 2010, respectively, in the Añamaza River and -8.9‰ and -6.9‰V-PDB in January and June 2010, respectively, in the Ebrón River).

The average $\delta^{18}\text{O}_{\text{water}}$ values from June and January are lower in the Añamaza River (-9.1 and -9.7‰ V-SMOW respectively) than in the Piedra (-8.5 and -8.6‰ V-SMOW) and Ebrón (-8.3 and -8.8‰ V-SMOW) Rivers, whose values are very similar (Table 1, Fig A2). The maximum individual $\delta^{18}\text{O}_{\text{water}}$ value (-7.3‰ V-SMOW) corresponds to the Piedra River values and the narrowest range of the individual values (-7.9 to -9.9‰ V-SMOW) corresponds to the Ebrón River (Table 1).

Six-month variation is barely displayed in the $\delta^{18}\text{O}_{\text{water}}$ evolution (Fig.4), with slightly lower values in January than in June (Fig. A2B and Table 1). The evolution through time shows a weak six-month pattern with many exceptions (Fig. 4). The pattern is slightly more distinct over the 12 year-period in the Piedra River (Osácar et al., 2013a). The evolutions over the synchronous monitoring time interval (2007 to Cool 2009-2010) are similar in the three rivers, except for the reversed observation in June 08, which is not reflected in the Añamaza River, and the remarkably low values in January 10, which are not reflected in the Piedra River.

Both $\delta^{13}\text{C}_{\text{DIC}}$ and $\delta^{18}\text{O}_{\text{water}}$ become higher downstream (Fig. 5), likely due, at least partially, to ongoing CO_2 outgassing, which is consistent with pCO_2 calculations based on hydrochemistry data. This downstream trend is clearer for $\delta^{18}\text{O}$ values in the three rivers and less clear for $\delta^{13}\text{C}_{\text{DIC}}$ values in the Añamaza and Ebrón Rivers (Fig. 5). Moreover, because the $\delta^{18}\text{O}_{\text{water}}$ values in the Piedra River correspond to sites that are approximately 12 km downstream of the springs (Fig 1C), the cumulative effect of CO_2 outgassing may be the reason that these values are higher in the Piedra River than in the Añamaza and Ebrón Rivers.

4.3 $\delta^{13}\text{C}_{\text{calcite}}$ and $\delta^{18}\text{O}_{\text{calcite}}$ values and patterns

In general, the differences in the average $\delta^{13}\text{C}_{\text{calcite}}$ values between the three rivers are minor, with those of the Piedra River being slightly lower (Figs. A3, 6 and Table 2). The average values of warm and cool periods are very similar in the three rivers (Fig. 6). The widest range corresponds to the Piedra River, while the ranges in the Añamaza and Ebrón Rivers are similar (Table 2). There is not a distinct six-month pattern in $\delta^{13}\text{C}$ (Figs. A3 and 7A), neither is the evolution of $\delta^{13}\text{C}$ parallel in the three rivers. Differences between facies A and C are obvious in the Ebrón River, with lower $\delta^{13}\text{C}$ values in facies C than in facies A (Fig. 6).

The Añamaza River exhibits the lowest $\delta^{18}\text{O}_{\text{calcite}}$ values, and the Piedra the highest values (Figs. A3, 6 and Table 2). In the three rivers, the $\delta^{18}\text{O}_{\text{calcite}}$ variation over time, with lower values in warm periods and higher values in cool periods, reflects six-month temperature variations, as expected based on the $\delta^{18}\text{O}$ temperature-dependent fractionation coefficient (Fig. A3 and 7B). The similarity between the six-month patterns of $\delta^{18}\text{O}$ in the Añamaza and Piedra Rivers is notable (Fig. A3). In the Ebrón River, the $\delta^{18}\text{O}$ values do not reflect the six-month periodicity to the same extent, and the differences between warm and cool periods are smaller (difference=0.04‰) than in the Añamaza River (difference=0.70‰) and the Piedra River (difference=0.81‰, for the same time interval and 0.72‰ for the 13-year record) (Table 2).

These differences in $\delta^{18}\text{O}_{\text{calcite}}$ between the three rivers are related to the different Tw values measured in each case. The most pronounced range of $\delta^{18}\text{O}_{\text{calcite}}$ six-month variability in the Piedra River (2.1‰V-PDB between maximum and minimum values) over the three-river common analysis intervals (Cool 2007-2008 to Cool 2009-2010) agrees with the largest six-month differences in mean Tw (5.4°C, Fig. A1). In the Añamaza and Ebrón Rivers, the six-month variability of $\delta^{18}\text{O}_{\text{calcite}}$ is smaller and proportional to their respective mean Tw ranges (the difference between maximum and

minimum values of $\delta^{18}\text{O}_{\text{calcite}}$ is 1.73‰V-PDB in the Añamaza River, with a range of 3.8°C in mean Tw, and 1.12‰V-PDB in the Ebrón River, with a range of 3.2°C in mean Tw). In the Ebrón River, which has the narrowest six-month, mean Tw range, the Cool 2007-2008 period does not display six-month temperature oscillations (Fig. A3 and 7B). There is little difference in $\delta^{18}\text{O}$ between facies A and C deposits in the Piedra and Ebrón Rivers. In the Añamaza River, the $\delta^{18}\text{O}$ values are lower in facies C than in facies A (Fig. 6). Nonetheless, the facies C record is incomplete in the three rivers (Fig. 7B). In the Piedra River, a general trend towards lower $\delta^{18}\text{O}_{\text{calcite}}$ values is displayed by most tablets throughout the 13-year monitoring period (Fig. A3).

4.4 Water temperature estimation

Water temperature estimation [Eq. 1] based on $\delta^{18}\text{O}_{\text{calcite}}$ and average $\delta^{18}\text{O}_{\text{water}}$ values (weighted mean for warm and cool periods) in each river yields values closer to the six-month average Tw than to the instant Tw (Fig. 8). Therefore, hereafter Tw refers to the mean water temperature of the six-month period, unless otherwise indicated.

Differences between the average calculated temperatures (mean of the calculated temperatures at all sites during every period in each river) and the average six-month Tw are always $\leq 2.7^\circ\text{C}$ (Table A3). The maximum average differences are 2.1°C for the Añamaza River, corresponding to the 2007-2008 period, 2.1°C for the Piedra River, corresponding to the Cool 2009-2010 period, and 2.7°C for the Ebrón River, corresponding to the Cool 2007-2008 period. The average difference between the calculated and recorded six-month Tw is 1.1°C in the Añamaza River (Cool 2007-2008 to Cool 2009-2010), 0.8°C in the Piedra River (2.6°C in the case of instantaneous temperatures; 2007-08 to Warm 2012) and 0.8°C in the Ebrón River (Cool 2007-2008 to Cool 2009-2010).

The observed differences between calculated and measured Tw are of the same order as those obtained in other recent tufas that likely correspond to systems close to oxygen isotopic equilibrium (Garnett et al., 2004; Leybourne et al., 2009; Brasier et al., 2010). The best fit is exhibited by the Piedra River. This fit is even more remarkable if the difference between actual and calculated Tw is compared with the measured Tw range in each river. This measured Tw range is larger in the Piedra River (5.4°C) than in the Añamaza and the Ebrón rivers (3.8°C and 3.2°C respectively).

5 Discussion

5.1 Isotopic fractionation

To assess the reliability of the isotopic composition of these tufa records as environmental archives, it is important to evaluate the isotopic fractionation in the calcite precipitation process.

Average $\delta^{13}\text{C}$ fractionation between calcite and dissolved bicarbonate is approximately $1 \pm 0.2\text{‰}$ regardless of temperature in the range of 10-40°C (Romanek et al., 1992; Garnett et al., 2004). In this study, $\delta^{13}\text{C}_{\text{DIC}}$ is lower than the corresponding average $\delta^{13}\text{C}_{\text{calcite}}$. This difference is larger in January (up to 2.0‰ in the Añamaza River) than in June (Tables 1 and 2). The difference between the average $\delta^{13}\text{C}_{\text{calcite}}$ and the average $\delta^{13}\text{C}_{\text{DIC}}$ ranges from a minimum of 0.40‰ in the Ebrón River in warm periods to a maximum of 2.01‰ in the Añamaza River in cool periods (Tables 1 and 2). In the Piedra River, this difference is approximately 1.3‰ both in warm and cool periods. These values are the same order of magnitude as those reported in other tufa studies (Matsuoka et al., 2001; Garnett et al., 2004; Kano et al., 2007; Lojen et al., 2009). Additionally, they suggest that carbon isotopic fractionation in the studied tufas is not far from isotopic equilibrium.

The actual fractionation coefficient of oxygen isotopes has been calculated from the $\delta^{18}\text{O}_{\text{calcite}}$ values and the average $\delta^{18}\text{O}_{\text{water}}$ values of the warm and cool periods and compared with the fractionation factors defined by Kim and O'Neil (1997), Coplen (2006) and Tremaine et al. (2011). In the three studied cases (Fig. 9), the actual fractionation coefficients are closer to the laboratory-based values reported by Kim and O'Neil (1997) than to those reported by Tremaine et al. and Coplen, which were based on cave studies, and than to the fractionation coefficients of Kele et al. (2015) for travertines and tufas. The coefficients of the studied cases here plot slightly above the Kim and O'Neil (1997) line and below the Tremaine et al. values, indicating a higher fractionation. This suggests that the actual fractionation of these tufa systems, despite not corresponding to a perfect isotopic equilibrium, is relatively homogeneous and is well represented by the equation used in the temperature estimation, which has already yielded good results when applied to this kind of tufa deposits (Arenas et al., 2010; Osácar et al., 2013a and b).

The slope of the Piedra River regression line is slightly lower than some of the other lines (Fig. 9) due to the warm periods exhibiting relatively higher fractionation than expected with respect to the cool periods. This effect has already been observed by Osácar et al. (2013a) in tufa sediment sampled in situ. This raises the question of the influence of the precipitation rate on the isotopic fractioning because, in general, isotopic equilibrium should be harder to reach at higher tufa precipitation rates (Tremaine et al., 2011, Watkins et al., 2014), which correspond to warm periods in the study cases (Arenas et al., 2014). The reason for this mismatch is not fully understood. Some studies have illustrated the complexity of the dependence of the isotopic fractionation on the deposition rate (DePaolo, 2011).

In summary, although some kinetic effects cannot be discarded, the fitting line of the actual fractionation in this study shows that the isotopic composition of the tufa calcite can be used to derive environmental information (e.g., T_w), in particular, in the case of the Piedra River. Nevertheless, the accuracy of T_w estimation based on the tufa record depends on the $\delta^{18}\text{O}_{\text{water}}$ composition, whose exact value for the whole six-month periods is unknown. The fractionation coefficient does not seem to be affected by the precipitation rate.

5.2 Temperature trends from $\delta^{18}\text{O}_{\text{calcite}}$ and air temperature

In addition to the estimation of the individual water temperatures, $\delta^{18}\text{O}_{\text{calcite}}$ can provide information regarding T_w evolution through time (Kano et al., 2007; Lojen et al., 2009).

In fossil tufa studies, this type of estimation is more common and, in general, the calculated T_w is assumed to reflect the regional T_{air} .

In the Piedra River, the T_w parallels the T_{air} from Cool 2007-2008 to Warm 2012 (Fig. 8). Most likely, the parallelism can be extended to the whole tufa record of this study (1999-2012). The T_{air} and measured T_w show a distinct increase from 1999 to 2012. According to the regression line, the T_{air} tendency increases from 12.4°C to 13.9°C (T_{air} change=1.5°C) and the calculated T_w increases from 13.1°C to 14.3°C (T_w change =1.2°C) in the case of facies C and from 13.2°C to 14.6°C (T_w change=1.4°C) in the case of facies A.

In other tufa deposits, the agreement between calculated and measured T_w is variable. In a 60-year record studied by Lojen et al. (2009) in Slovenia, trends of calculated and measured temperatures differ significantly because of the kinetic effects associated with isotope fractionation. In the 15-year tufa record studied by Kano et al. (2007), the calculated temperatures agreed with the measured temperatures. This agreement was

attributed to the stability of the water isotopic signature based on the residence time of water in the aquifer. In the Piedra River, because the river $\delta^{18}\text{O}_{\text{water}}$ is not fully stable (Fig. 4 and Table 1), the weak six-month variation in $\delta^{18}\text{O}_{\text{water}}$ has been accounted for in the Tw estimation (using averaged $\delta^{18}\text{O}_{\text{water}}$ values for warm and cool periods). The results prove that the $\delta^{18}\text{O}_{\text{calcite}}$ values mimic the evolution of Tair with a reasonable reliability (Fig. 8B). Although the trend line of the calculated Tw is always slightly higher ($\sim 1.5^\circ\text{C}$) than the Tair line, the parallelism between Tair and calculated Tw shows that the calculated Tw tendency is reliable and, generally, is more useful for fossil tufa analyses than the Tw estimation itself.

Over the interval Cool 2007-2008 to Cool 2009-2010, comparisons between the calculated Tw, the average six-month Tw and Tair in the three rivers yield dissimilar results. In the Piedra River, Tair exhibits an increasing tendency (Fig. 8D), similar to the actual Tw trend. The $\delta^{18}\text{O}_{\text{calcite}}$ -derived Tw tendency also increases, but the slope is much higher. This discrepancy may be due to the small number of periods considered compared to the 13-year record.

In the Añamaza River Tair exhibits a slight increase throughout the 3-year record, whereas the measured Tw and the calculated Tw decrease during the same time interval. Temperatures calculated from facies C are slightly higher than actual Tw. In contrast, calculations from facies A are slightly lower than the actual Tw and closer to Tair (Fig. 8A). These differences may be related to the offset of approximately 2°C between the Tw and Tair.

The differences in $\delta^{18}\text{O}_{\text{calcite}}$ between facies A and C (Figs. 6 and 7) do not have a major influence on the estimated Tw, which show very small differences between these facies. Nevertheless, facies A seems more suitable for temperature estimation because it shows a more complete record.

In the Ebrón River, both the measured and the calculated Tw exhibit decreasing trends, whereas the Tair are mostly invariable (Fig. 8C). In this river, the seasonal oscillation in actual Tw is significantly narrower than in the other rivers, especially during cool periods when average Tw can be up to 8°C higher than Tair. Consequently, both the measured and calculated Tw tendencies yield much higher values than Tair. The Tair variations are not apparent in the river Tw, likely due to the diffuse groundwater inputs along the river (Arenas et al., 2015).

Despite the differences between measured and calculated Tw, the Tw trends are more reliable than the temperature itself. The calculated Tw can reflect the Tair if the analysed time interval is long enough and if the hydrologic conditions allow the Tair signature to be transferred to the river water. The best fit between calculated Tw and Tair tendencies corresponds to the 13-year record of the Piedra River.

5.3 Caveats regarding the water temperature estimation from tufa $\delta^{18}O$

From the comparison between the temperature estimation results in the three rivers, some caveats arise, other than the ones derived from the isotopic fractionation process. The effect of the different $\delta^{18}O_{\text{water}}$ values on Tw estimation from $\delta^{18}O_{\text{calcite}}$ is illustrated by the Añamaza River. These differences can be mistaken for changes in temperature. This river exhibits the lowest $\delta^{18}O_{\text{calcite}}$ values (Fig. 6), which may be the result of a higher calcite precipitation temperature. However, this river exhibits the lowest Tw of the three rivers (Fig. A1). Therefore, the low $\delta^{18}O_{\text{water}}$ values of the Añamaza River water (Fig. 4) result in these low $\delta^{18}O_{\text{calcite}}$ values. These low $\delta^{18}O_{\text{calcite}}$ values reflect the influence of both the $\delta^{18}O_{\text{water}}$ composition and the temperature fractionation effects. The change in $\delta^{18}O_{\text{water}}$ composition is the reason for some Quaternary tufa $\delta^{18}O$ variation (Garnett et al., 2004; Brasier et al., 2010). In these cases, the $\delta^{18}O_{\text{calcite}}$ values

reveal the isotopic signature of rainfall, which, through aquifer recharge, is transferred to the river water and, subsequently, to tufa calcite (Garnett et al., 2004; Liu et al., 2006). Estimating regional T_{air} based on the Añamaza River $\delta^{18}O_{calcite}$ would result in temperature overestimation.

The Ebrón River represents another example of potentially misinterpreted climate conditions. The small $\delta^{18}O_{calcite}$ difference between warm and cool periods in the Ebrón River (Fig. 6) is related to the small difference in T_w between cool and warm periods (Fig. 5 and A1). However, these T_w differences do not respond to smaller seasonal T_{air} oscillations in the area. This feature is likely associated with continuous groundwater inputs at several points along the monitored river stretch (Arenas et al., 2015). These inputs diminish the influence of T_{air} on the seasonal changes in T_w and, thus, are responsible for the weak response of the tufa record to T_{air} changes. Estimating regional T_{air} based on the Ebrón River tufa would underestimate the six-month contrast.

These findings suggest that although the three studied rivers are located in the same geographic and climatic context, the corresponding tufa isotopic record can vary due to differences in local environmental and hydrogeological features (see below). In the case of fossil tufa studies, disregarding these phenomena may result in misinterpretation of regional temperatures, even in the cases in which the isotopic fractionation is close to equilibrium.

6. Comparison between the three rivers: discerning local and regional changes

The differences shown by the isotopic record of the three river tufas give evidence of the importance of considering the local and regional hydrological differences in the studies of paleoclimate based on $\delta^{18}O$.

Changes in $\delta^{13}\text{C}_{\text{calcite}}$ and $\delta^{18}\text{O}_{\text{calcite}}$ between close tufa-depositing streams in a region or in a basin can be related to differences in the isotopic compositions of rainfall and springs feeding the streams, and to differences in the discharge and distribution of groundwater inputs along the stream. In addition, varying aquifer residence times can also induce changes in the calcite isotopic composition (Garnett et al., 2004; Andrews, 2006; Liu et al., 2006). The rivers studied in the Iberian Range are suitable for discerning the influences of such parameters and factors on the calcite isotopic composition.

6.1 Groundwater isotopic composition and discharge

$\delta^{18}\text{O}_{\text{water}}$ variations along the Ebrón River are not large, relative to the studied stretch (22 km, Table A1), likely because of the groundwater inputs along its path result in small $\delta^{18}\text{O}_{\text{water}}$ variations along the studied stretch (Fig. 5C). In the Añamaza River (in a 18km stretch), the effects of downstream ^{18}O -enrichment are larger than in the Ebrón River (Fig. 5A).

In the Piedra River, $\delta^{18}\text{O}_{\text{water}}$ values of the main spring (Fig. 1) are distinctly higher in June than in January (Fig. 3), which is consistent with the seasonal variation of rainfall $\delta^{18}\text{O}$ (i.e., lower in the cool season than in the warm season; Sharp, 2007, sect. 4.7.1). The river $\delta^{18}\text{O}_{\text{water}}$ evolution throughout the 12-year study shows a much less distinct temporal pattern (Figs. 3 and 4).

The average $\delta^{13}\text{C}_{\text{calcite}}$ values of the Piedra River parallel the $\delta^{13}\text{C}_{\text{DIC}}$ values of the main springs (Fig. 3), significantly lower than those of the Añamaza and Ebrón rivers. Therefore, the slight $\delta^{13}\text{C}_{\text{calcite}}$ variations found in the different studied sites along this river may be due to local phenomena that do not respond to regional environmental conditions.

In both the Ebrón and Añamaza Rivers, the discharge maxima coincide with low river $\delta^{18}\text{O}_{\text{water}}$ values. This relationship is observed in January 2010 in both rivers and in June 08 in the Ebrón River (Fig. 10A, C). Both the June 2008 and January 2010 peaks coincide with increased rainfall phenomena (Fig. 10A, C). However, the corresponding $\delta^{18}\text{O}_{\text{calcite}}$ values barely mark these high discharge and rainfall phenomena. These were likely unique episodes (Auqué et al., 2014), the effects of which were concealed in the six-month period deposits and because if the event occurred during the coldest month, tufa deposition would not have been favoured (cf., Hori et al., 2009; Brasier et al., 2010; Auqué et al., 2014). Moreover, in the Añamaza River, high discharge events caused dilution in the river water (Auqué et al., 2014) and partial erosion of the tufa deposits. In the Ebrón River, lower deposition rates correlate with high discharge episodes (Arenas et al., 2015). Therefore, although in both rivers the river $\delta^{18}\text{O}_{\text{water}}$ reflects changes in rainfall and discharge, the $\delta^{18}\text{O}_{\text{calcite}}$ record does not reflect these changes. In turn, $\delta^{13}\text{C}_{\text{calcite}}$ does not exhibit parallelism with either discharge or rainfall (Fig. 10A, B).

Unlike the Añamaza and Ebrón Rivers, the Piedra River $\delta^{18}\text{O}_{\text{water}}$ values are not directly related to discharge variations, and precipitation does not parallel discharge. Only certain high discharge events (e.g., June 2008) are accompanied by precipitation maxima (Fig. 10C). The delay between rainfall and its signature in the river water isotopic composition was previously noted by Osácar et al. (2013a) and explained by aquifer storage, which occurs in other tufa systems (Ihlenfeld et al., 2003).

In turn, the $\delta^{13}\text{C}_{\text{calcite}}$ values in the Piedra River mimic discharge variations, particularly in the case of facies A ($r=-0.42$, $N=26$) (Fig. 10B). The $\delta^{13}\text{C}_{\text{calcite}}$ values are higher from Cool 1999-2000 to Warm 2003, which is an interval of especially low discharge. From Cool 2003-2004 to 2009, certain higher discharge values coincide with low $\delta^{13}\text{C}_{\text{calcite}}$ values. The discharge decrease from Cool 2011-2012 to Warm 2012 coincides with an

increase in $\delta^{13}\text{C}_{\text{calcite}}$, which was detected in both facies. This reverse correlation between discharge and $\delta^{13}\text{C}_{\text{calcite}}$ has been observed in other tufa deposits in which high values of $\delta^{13}\text{C}_{\text{calcite}}$ are linked to low discharge periods due to long aquifer residence times and consequent ^{13}C -enrichment (Makhnatch et al., 2004; Garnett et al., 2004).

6.2 $\delta^{18}\text{O}$ composition of precipitation

Variations in rainfall $\delta^{18}\text{O}_{\text{water}}$ can contribute to differences in tufa $\delta^{18}\text{O}_{\text{calcite}}$ (Andrews et al., 1994; Wang et al., 2014). An example of the influence of rainfall $\delta^{18}\text{O}_{\text{water}}$ on river $\delta^{18}\text{O}_{\text{water}}$ is the six-month variation observed in the groundwater $\delta^{18}\text{O}$ signature in the Piedra River (Fig. 3). This variation is likely due to the seasonal variation of rainfall $\delta^{18}\text{O}$, which is lower in winter.

The lower $\delta^{18}\text{O}_{\text{water}}$ values in the Añamaza River compared to the other two rivers (Fig. A2B) cannot be explained by latitudinal differences between the three rivers, as these are small and appear to have no influence on general tufa development (Sancho et al., 2015). Temperature differences are also not responsible because T_{air} of cool periods in the Añamaza River is slightly higher than T_{air} during cool periods in the Ebrón River. Altitude is also not the cause, as the drainage areas of the three rivers are slightly above 1000 m a.s.l., and only the studied stretch of the Piedra River is at a lower altitude (786 m a.s.l.).

The location of the rivers between the Atlantic Ocean and the Mediterranean Sea may explain such differences. This type of moisture source variation has been used to explain the $\delta^{18}\text{O}$ variations of Quaternary tufas in the SE Iberian Ranges (Domínguez-Villar et al., 2014). The rainfall $\delta^{18}\text{O}$ values on the Atlantic coast are generally lower than those on the Mediterranean coast based on the long-term weighted $\delta^{18}\text{O}$ precipitation values from the Santander (-6.1‰ V-SMOW) and Valencia (-5.0‰ V-

SMOW) stations (Araguás-Araguás and Díaz-Teijeiro, 2005). The location of the Añamaza River catchment, which is closer to the Atlantic Ocean than the Piedra and Ebrón Rivers, results in a larger proportion of ^{18}O -depleted rainfall in the area compared to the two other areas. The mean rainfall values of the GNIP stations of Soria (-7.7‰ V-SMOW, year 2003), Madrid and Zaragoza (-6.3‰ V-SMOW, years 2000 to 2009 in both cases), which may be used as proxies of the rainfall sources for these rivers, illustrates this situation. However, the lack of data of $\delta^{18}\text{O}$ of the river catchment areas and of the behavior of the aquifers only allow a qualitative approaching to this issue.

This result suggests that the Añamaza River water reflects, to some extent, the rainfall $\delta^{18}\text{O}_{\text{water}}$ signature (Fig. 4). However, this signature is only partially transmitted to $\delta^{18}\text{O}_{\text{calcite}}$. In this river, the $\delta^{18}\text{O}_{\text{calcite}}$ values are lower than those in the Piedra and Ebrón Rivers in warm periods, but not in cool periods, when the isotopic fractionation under lower temperatures favours a higher $\delta^{18}\text{O}_{\text{calcite}}$.

Therefore, the Piedra and Ebrón rivers do not maintain full $\delta^{18}\text{O}$ signature of the rainfall, as does the Añamaza River. The delayed influence of rainfall on the river water $\delta^{18}\text{O}$ signature in the case of the Piedra River and the repeated groundwater inputs in the Ebrón River may be the causes of such differences.

These findings suggest that even rivers in close proximity can display different behaviours relative to their tufa stable isotope signatures. Rainfall, aquifer residence time, $\delta^{13}\text{C}$ composition of the aquifer groundwater and groundwater inputs along the river may cause different isotopic signatures in tufa in close depositional areas.

7. Comparison with other tufa profiles

Since Matsuoka et al. (2001) showed that tufa $\delta^{18}\text{O}$ and $\delta^{13}\text{C}$ reflected the seasonal variations of Tw and DIC content, many papers have dealt with the climatic significance

of tufa stable isotopes, but there are very few published works that cover periodical analysis of environmental parameters and the correlative sediment records through long time spans.

In the Mediterranean context, only Lojen et al. (2009) studied a 60-year profile of tufa, formed inside a tunnel, linked to a dam of the river, in Slovenia. The presence of non-equilibrium precipitation of calcite and the complicated hydrological situation hampered the relation between temperature and calcite $\delta^{18}\text{O}$; nevertheless, calcite $\delta^{18}\text{O}$ conforms to river discharge since 1981. In contrast, in the studied cases in the Iberian Peninsula, the discharge does not correlate with $\delta^{18}\text{O}_{\text{calcite}}$, and only $\delta^{18}\text{O}_{\text{water}}$ decreases with high discharge events in the Añamaza and Ebrón rivers, but not in the Piedra River.

In the Iberian cases, the $\delta^{18}\text{O}_{\text{calcite}}$ independence of the discharge events favors that $\delta^{18}\text{O}_{\text{calcite}}$ can reflect more accurately the T_w . These varying results highlight the importance of the hydrological characteristics to the carbonate isotopic signature.

In Greece, Brasier et al. (2010) studied a Holocene tufa stromatolite profile and compared the tufa $\delta^{18}\text{O}$ -derived water temperatures with the ones obtained from recent tufa $\delta^{18}\text{O}$ that formed in isotopic equilibrium. However, the calculated temperature range of the Holocene tufa corresponded only to autumn and spring, the only seasons when tufa forms in this case, which coincided with sharp textural changes between the successive laminæ. In the three studied rivers of the Iberian Peninsula, although the tufa formation rate depends on the season (i.e., Warm and Cool periods), no systematic hiatuses have been inferred. Besides, the tufa sampling method intended that samples would represent the whole Warm and Cool periods. The actual T_w range is similar to the measured T_w , which supports that tufa formation occurs through the whole year, although the estimated temperatures are always higher, which is explained by the fostering of tufa formation by higher temperatures. Accordingly, the $\delta^{18}\text{O}_{\text{calcite}}$ ranges in

the continuous records of the Iberian tufas are wider than the range in the Greek tufa with the partial record.

Other studied tufa profiles correspond to monsoon or subtropical climates, where heavy rainfall dominates part of the year. In these cases, the heavy rain can dilute the original water $\delta^{13}\text{C}_{\text{water}}$ and $\delta^{18}\text{O}_{\text{water}}$ signature and the tufa isotopic record can reflect the heavy rain episodes or season as a decrease in $\delta^{13}\text{C}$, $\delta^{18}\text{O}$ or both (Liu et al., 2006). When rainy seasons alternate with droughts, evaporation can cause variability in the tufa stable isotope signature, as in the 14-year profile of recent tufa of Australia, formed under a semiarid monsoon climate, studied by Ihlenfeld et al. (2003). In that case the long residence time of water (1.5 years) in the aquifer can delay and blur this effect. In the Piedra River, although rainfall is not so intense, the decreasing of $\delta^{13}\text{C}_{\text{calcite}}$ with discharge increase is also observed, likely because the water residence time is smaller.

Another example is the 15-year tufa profile studied by Kano et al. (2007), from the subtropical Miyako Island, southern Japan, that experiences intense rainy periods and droughts. The calcite $\delta^{18}\text{O}$ record reflects the air temperature trend through the 15-year period, although the estimated temperature change is more than twice the measured change, which, according to the authors, may be due to a change in $\delta^{18}\text{O}_{\text{water}}$. In the case of the Piedra River, the difference between calculated and measured T_w is much smaller and the available water $\delta^{18}\text{O}_{\text{water}}$ shows no significant variations through the studied period.

In none of the referred cases is there a record of water characteristics (temperature, hydrochemistry, $\delta^{18}\text{O}$) synchronous to the tufa deposition, as in the case of the Iberian Range rivers. This validation makes the results of these rivers (three different rivers along a 200-km long transect, a large number of samples and long time spans),

significant and relevant to interpreting climatic parameters from stable isotopes of continental carbonate systems.

8 Conclusions

A comparison of $\delta^{13}\text{C}$ and $\delta^{18}\text{O}$ in recent tufa (stromatolite and moss and algal boundstones deposited on artificial substrates and monitored periodically from 3 to 13 years) from three rivers (Añamaza, Piedra and Ebrón Rivers along a 200-km N-S transect in NE Spain) has yielded the following important conclusions:

- Calcite precipitation occurred close enough to equilibrium for certain environmental information to be derived from the tufa isotopic composition.
- The $\delta^{18}\text{O}_{\text{calcite}}$ values of the three rivers display cyclic variation (six-month variation), which is consistent with the six-month T_w variation and is mainly due to temperature-dependent isotopic fractionation.
- Average six-month T_w estimated from the $\delta^{18}\text{O}_{\text{calcite}}$ and the mean $\delta^{18}\text{O}_{\text{water}}$ values of the cool and warm seasons in each river differ from the corresponding actual T_w by less than 2.7°C. An even better agreement is found between the tendencies of the calculated T_w and the T_{air} . The best agreement corresponds to the 13-year Piedra River record; over this period, an increase of 1.3°C in calculated T_w corresponds to an actual T_{air} warming of 1.5°C.
- The tufa $\delta^{13}\text{C}$ values do not exhibit distinct patterns; however, in the Piedra River, the $\delta^{13}\text{C}_{\text{DIC}}$ reflects the spring water $\delta^{13}\text{C}_{\text{DIC}}$ signature and the only variation is the downstream increase by the outgassing of ^{13}C -depleted CO_2 . Tufa stromatolites prove to be the most suitable sedimentary facies for estimating regional temperatures.

Differences in the $\delta^{18}\text{O}_{\text{calcite}}$ record across the studied 200-km transect cannot be attributed to temperature changes, but they are due to variable influences of groundwater inputs and isotopic rainfall composition at each site.

- Lower $\delta^{18}\text{O}$ values of rainfall yield lower $\delta^{18}\text{O}_{\text{calcite}}$ values that can be misinterpreted as being due to higher regional temperatures. Permanent groundwater inputs along the rivers diminish the influence of Tair on river Tw and their seasonal variations. The ensuing smaller range in $\delta^{18}\text{O}_{\text{calcite}}$ values may be misinterpreted as a smaller seasonal temperature variation.
- In rivers mainly fed by groundwater at the headwaters and that exhibit a delay between precipitation and corresponding discharge variation, the river $\delta^{18}\text{O}_{\text{water}}$ keeps the signature of rainfall $\delta^{18}\text{O}_{\text{water}}$ composition only partially. Consequently, these conditions provide a suitable scenario for climate interpretation based on tufa stable isotope composition.

These findings highlight the importance of accounting for both groundwater behaviour and rainfall stable isotope composition when interpreting climate parameters from stable isotope compositions in carbonate systems, particularly when differences in the isotopic signatures of deposits exist in the same region.

7 Acknowledgements

This study was funded by the REN2002-03575/CLI, CGL2006-05063/BTE, CGL2009-09216/CLI and CGL2013-42867-Projects of the Spanish Government and European Regional Funds. This work is a contribution of the *Continental Sedimentary Basins Analysis, Geotransfer, PaleoQ* and *GMG* (Aragón Government and University of Zaragoza) research groups. We thank the personnel of the *Servicio de Preparación de Rocas y Materiales Duros* and Scanning Electron Microscopy (*Servicio General de*

Apoyo a la Investigación-SAI) of the University of Zaragoza for their technical help. We are grateful to the management and staff of the Monasterio de Piedra Natural Park for facilitating our fieldwork. We are also grateful to the anonymous reviewers and the editor for their valuable comments.

References

- Andrews, J.E., 2006. Palaeoclimatic records from stable isotopes in riverine tufas: Synthesis and review. *Earth-Sci. Rev.* 75, 85-104.
- Anzalone, E., Ferreri, V., Sprovieri, M., D'Argenio, B., 2007. Travertines as hydrologic archives: The case of the Pontecagnano deposits (southern Italy). *Adv. Water Resour.* 30, 2159-2175.
- Araguás-Araguás L.J., Díaz Teijeiro, M.F., 2005. Isotope composition of precipitation and water vapour in the Iberian Peninsula. In: *Isotopic composition of precipitation in the Mediterranean Basin in relation to air circulation patterns and climate*, IAEA, Isotope Hydrology Section. Vienna, Austria, 173–191.
- Arenas, C., Osácar, C., Sancho, C., Vázquez-Urbez, M., Auqué, L. and Pardo, G., 2010. Seasonal record from recent fluvial tufa deposits (Monasterio de Piedra, NE Spain): sedimentological and stable isotope data. In: *Tufas and Speleothems: Unravelling the Microbial and Physical Controls* (Eds H.M. Pedley and M. Rogerson), Geological Society, London, 119–142.
- Arenas, C., Vázquez-Úrbez, M., Auqué, L., Sancho, C., Osácar, M.C., Pardo, G., 2014. Intrinsic and extrinsic controls of spatial and temporal variations in modern fluvial tufa sedimentation: A thirteen-year record from a semi-arid environment. *Sedimentology* 61, 90–132. doi: 10.1111/sed.12045

- Arenas, C., Auqué, L., Osácar, M.C., Sancho, C., Lozano, M.V., Vázquez-Urbez, M., Pardo, G., 2015. Current tufa sedimentation in a high discharge river: A comparison with other synchronous tufa records in the Iberian Range (Spain). *Sediment. Geol.* 325 132–157. <http://dx.doi.org/10.1016/j.sedgeo.2015.05.007>
- Auqué, L., Arenas, C., Osácar, C., Pardo, G., Sancho, C., Vázquez-Urbez, M., 2013. Tufa sedimentation in changing hydrological conditions: the River Mesa (Spain). *Geol. Acta* 11, 85–102.
- Auqué, L., Arenas, C., Osácar, C., Pardo, G., Sancho, C., Vázquez-Urbez, M., 2014. Current tufa sedimentation in a changing-slope valley: the River Añamaza (Iberian Range, NE Spain). *Sediment. Geol.* 303, 26–48.
- Brasier, A.T., Andrews, J.E., Marca-Bell, A.D., Dennis, P.F., 2010. Depositional continuity of seasonally laminated tufas: Implications for $\delta^{18}\text{O}$ based palaeotemperatures. *Global Planet. Change* 71, 160–167. doi:10.1016/j.gloplacha.2009.03.022
- Capezzuoli, E., Gandin, A., Pedley, M., 2014. Decoding tufa and travertine (fresh water carbonates) in the sedimentary record: The state of the art. *Sedimentology* 61, 1–21.
- Chafetz, H.S., Utech, N.M., Fitzmaurice, S.P., 1991. Differences in the $\delta^{18}\text{O}$ and $\delta^{13}\text{C}$ signatures of seasonal laminae comprising travertine stromatolites. *J. Sediment. Petrol.* 61, 1015–1028.
- Chen, J., Zhang, D.D., Wang, S., Xiao, T., Huang, R., 2004. Factors controlling tufa deposition in natural waters at waterfall sites. *Sediment. Geol.* 166, 353–366.
- Coplen, T., 2007. Calibration of the calcite-water-oxygen isotope geothermometer at Devils Hole, Nevada, a natural laboratory. *Geochim. Cosmochim. Acta* 71, 3948–3957.

- DePaolo, D.J., 2011. Surface kinetic model for isotopic and trace element fractionation during precipitation of calcite from aqueous solutions. *Geochim. Cosmochim. Acta* 75, 1039–1056.
- Domínguez-Villar, D., Vázquez-Navarro, J.A., Carrasco, R.M., 2012. Mid-Holocene erosive episodes in tufa deposits from Trabaque Canyon, central Spain, as a result of abrupt arid climate transitions. *Geomorphology* 161–162, 15–25. doi:10.1016/j.geomorph.2012.03.028
- Garnett, E.R., Andrews, J.E., Preece, R.C., Dennis, P.F., 2004. Climatic change recorded by stable isotopes and trace elements in a British Holocene tufa. *J. Quat. Sci.* 19(3) 251–262 DOI: 10.1002/jqs.842
- Gradzinski, M., 2010. Factors controlling growth of modern tufa; results of a field experiment. In: Pedley, M., and Rogerson, M. eds., *Tufas and Speleothems: Unravelling the Microbial and Physical Controls* 61, Geological Society, London, 133–175.
- Hori, M., Kawai, T., Matsuoka, J., and Kano, A., 2009. Intra-annual perturbations of stable isotopes in tufas; effects of hydrological processes. *Geochim. Cosmochim.* 73, 1684–1695.
- Ihlenfeld, C., Norman, M.D., Gagan, M.K., Drysdale, R.N., Maas, R., and Webb, J., 2003. Climatic significance of seasonal trace element and stable isotope variations in a modern freshwater tufa. *Geochim. Cosmochim.* 67, 2341–2357.
- Kano, A., Kawai, T., Matsuoka, J., Ihara, T., 2004. High-resolution records of rainfall events from clay bands in tufa. *Geology* 32, 793–796.
- Kano, A., Hagiwara, R., Kawai, T., Hori, M., Matsuoka, J., 2007. Climatic conditions and hydrological change recorded in a high-resolution stable-isotope profile of a

- recent laminated tufa on a subtropical island, southern Japan. *J. Sediment. Res.* 77, 59-67.
- Kele, S, Breitenbach, S.F.M., Capezzuoli, E., Meckler, A.N., Ziegler, M., Millan, I.M., Kluge, T., Deák, J., Hanselmann, K., John, C.M., Yan, H., Liu, Z., Bernasconi, S.M., 2015. Temperature dependence of oxygen- and clumped isotope fractionation in carbonates: A study of travertines and tufas in the 6–95 °C temperature range. *Geochim. Cosmochim.* 168, 172–192. <http://dx.doi.org/10.1016/j.gca.2015.06.032>
- Kim, S.-T., and O'Neil, J.R., 1997. Equilibrium and non-equilibrium oxygen isotope effects in synthetic carbonates. *Geochim. Cosmochim.* 61, 3461-3475.
- Leybourne, M.I., Betcher, R.N., McRitchie, W.D., Kaszycki, C.A., Boyle, D.R., 2009. Geochemistry and stable isotopic composition of tufa waters and precipitates from the Interlake Region, Manitoba, Canada. Constraints on groundwater origin, calcitization, and tufa formation. *Chem. Geol.* 260, 221-233.
- Liu, Z., Svensson, U., Dreybrodt, W., Yuan, D., and Buhmann, D., 1995. Hydrodynamic control of inorganic calcite precipitation in Huanglong Ravine, China: Field measurements and theoretical prediction of deposition rates. *Geochim. Cosmochim.* 59, 3087-3097.
- Liu, Z., Li, H., You, C., Wan, N., Sun, H., 2006. Thickness and stable isotopic characteristics of modern seasonal climate-controlled sub-annual travertine laminae in a travertine-depositing stream at Baishuitai, SW China: implications for paleoclimate reconstruction. *Environ Geol* 51, 257–265. DOI 10.1007/s00254-006-0323-0
- Liu, Z., Sun, H., Baoying, L., Xiangling, L., Wenbing, Y., Cheng, Z., 2010. Wet-dry seasonal variations of hydrochemistry and carbonate precipitation rates in a travertine-depositing canal at Baishuitai, Yunnan, SW China: Implications for the

- formation of biannual laminae in travertine and for climatic reconstruction. *Chem. Geol.* 273, 258–266. doi:10.1016/j.chemgeo.2010.02.027
- Lojen, S., Dolenc, T., Vokal, B., Cukrov, N., Mihelci, G., Papesch, W., 2004. C and O stable isotope variability in recent freshwater carbonates (River Krka, Croatia). *Sedimentology* 51, 361-375.
- Lojen, S., Trkov, A., Scancar, J., Vazquez-Navarro, J.A., Cukrov, N. 2009, Continuous 60 year stable isotopic and earth-alkali element records in a modern laminated tufa (Jaruga, River Krka, Croatia); implications for climate reconstruction. *Chem. Geol.* 258, 242-250.
- Makhnach, N., Zernitskaja, V., Kolosov, I., Simakova, G., 2004. Stable oxygen and carbon isotopes in Late Glacial–Holocene freshwater carbonates from Belarus and their palaeoclimatic implications. *Palaeogeogr. Palaeoclimatol. Palaeoecol.* 209, 73–101. doi:10.1016/j.palaeo.2004.02.019
- Manzo, E., Perri, E., and Tucker, M.E., 2012. Carbonate deposition in a fluvial tufa system: processes and products (Corvino Valley – southern Italy). *Sedimentology* 59, 553–577.
- Matsuoka, J., Kano, A., Oba, T., Watanabe, T., Sakai, S., Seto, K., 2001. Seasonal variation of stable isotopic compositions recorded in a laminated tufa, SW Japan. *Earth Planet. Sci. Lett.* 192, 31-44.
- O'Brien, G.R., Kaufman, D.S., Sharp, W.D., Atudorei, V., Parnell, R.A., Crossey, L.J., 2006. Oxygen isotope composition of annually banded modern and mid-Holocene travertine and evidence of paleomonsoon floods, Grand Canyon, Arizona, USA. *Quatern. Res.* 65, 366–379.
- Osácar, C., Arenas, C., Vázquez-Urbez, M., Sancho, C., Auqué, L.F., Pardo, G., 2013a. Environmental factors controlling the $\delta^{13}\text{C}$ and $\delta^{18}\text{O}$ variations of recent fluvial tufas:

- a 12-year record from the Monasterio de Piedra Natural Park (NE Iberian Peninsula).
J. Sediment. Res.83, 309–322.
- Osácar, C., Arenas, C., Vázquez-Urbez, M., Sancho, C., Auqué, L.F., Pardo, G., Lojen, S and Cukrov, N., 2013b. Seasonal and decadal stable isotope evolution recorded by recent tufa deposited on artificial substrates in the Monasterio de Piedra Natural Park (NE Spain). *Geogaceta* 54, 135-138.
- Pedley, M., 2009. Tufas and travertines of the Mediterranean region: a testing ground for freshwater carbonate concepts and developments. *Sedimentology* 56, 221–246.
- Peña, J.L., Sancho, C., Arenas, C., Auqué, L., Longares, L.A., Lozano, M.V., Meléndez, A., Osácar, C., Pardo, G., Vázquez-Urbez, M., 2014. Las tobas cuaternarias en el sector aragonés del sistema ibérico. In: *Las Tobas en España. Serie monografías*. Eds: González Amuchastegui, M.J. & González Martín, J.A. Sociedad Española de Geomorfología Monografía 12, 159-172.
- Romanek, C.S., Grossman, E.L., Worsé, J.W., 1992. Carbon isotopic fractionation in synthetic aragonite and calcite: Effects of temperature and precipitation rate. *Geochim. Cosmochim. Acta*56, 419-430.
- Sancho, C., Arenas, C., Vázquez-Urbez, M., Pardo, G., Lozano, M.V., Peña, J.L., Hellstrom, J., Ortiz, J.E., Osácar, M.C., Auqué, L., Torres, T. 2015. Climatic implications of the Quaternary fluvial tufa record in the NE Iberian Peninsula over the last 500 ka. *Quatern. Res.* 84 (3), 398–414.
<http://dx.doi.org/10.1016/j.yqres.2015.08.003>.
- Sharp, Z. 2007. *Principles of Stable Isotope Geochemistry*. Pearson Prentice Hall, New Jersey, U.S.A,

- Sun, H., Liu, Z., Yan, H., 2014. Oxygen isotope fractionation in travertine-depositing pools at Baishuitai, Yunnan, SW China: Effects of deposition rates. *Geochim. Cosmochim. Acta* 133, 340–350. <http://dx.doi.org/10.1016/j.gca.2014.03.006>
- Tremaine, D.M., Froelich, P.N., Wang, Y., 2011. Speleothem calcite farmed *in situ*: Modern calibration of $\delta^{18}\text{O}$ and $\delta^{13}\text{C}$ paleoclimate proxies in a continuously-monitored natural cave system. *Geochim. Cosmochim. Acta* 75, 4929–4950. doi:10.1016/j.gca.2011.06.005
- Vázquez-Urbez, M., Arenas, C., Sancho, C., Osácar, C., Auqué, L., and Pardo, G., 2010. Factors controlling present-day tufa dynamics in the Monasterio de Piedra Natural Park (Iberian Range, Spain): depositional environmental settings, sedimentation rates and hydrochemistry: *International Journal of Earth Sciences*, v. 99, p. 1027-1049.
- Vázquez-Urbez, M., Arenas, C., Sancho, C., Auqué, L.F., Osácar, M.C., and Pardo, G., 2011. Quaternary and present-day tufa systems of the Rivers Piedra and Añamaza (Iberian Range, Spain). In: Arenas, C., Pomar, L. and Colombo, F., eds., *Geo-Guías 8 Post-Meeting Field Trips, 28th IAS Meeting, Zaragoza, Sociedad Geológica de España*, 241-274.
- Wang, H., Yan, Y., Liu, Z., 2014. Contrasts in variations of the carbon and oxygen isotopic composition of travertines formed in pools and a ramp stream at Huanglong Ravine, China: Implications for paleoclimatic interpretations. *Geochim. Cosmochim. Acta* 125, 34–48. <http://dx.doi.org/10.1016/j.gca.2013.10.001>
- Watkins, J.M., Hunt, J.D., Ryerson, F.J., and DePaolo, D.J., 2014. The influence of temperature, pH, and growth rate on the $\delta^{18}\text{O}$ composition of inorganically precipitated calcite. *Earth and Planetary Science Letters* 404, 332–343. <http://dx.doi.org/10.1016/j.epsl.2014.07.036>

Yan, H., Sun, H., Liu, Z., 2012. Equilibrium vs. kinetic fractionation of oxygen isotopes in two low-temperature travertine-depositing systems with differing hydrodynamic conditions at Baishuitai, Yunnan, SW China. *Geochim. Cosmochim. Acta* 95, 63–78. <http://dx.doi.org/10.1016/j.gca.2012.07.024>

Figure and table captions

Fig. 1. Location and geological setting of the studied rivers. (A) Geographical location. (B) to (E) Geological maps of the three studied rivers with locations of tablet sites and water sampling points. (B) Ebrón River, (C, D) Piedra River, (E) Añamaza River. Modified from Auqué et al. (2014) and Arenas et al. (2014, 2015).

Fig. 2. Depositional subenvironments and sedimentary facies studied. (A) Fast-flowing water area devoid of macrophytes in which Facies A forms. (B) Cross-section of tablet P-14 (Facies A) indicating six-month intervals. (C) Scanning electron microscope image of Facies A showing calcite tubes mostly subperpendicular to lamination that form a palisade. (D) Stepped waterfall with moss and algae in which Facies C and minor Facies A form. Position of tablet P-11 for sedimentation monitoring is circled. (E) Cross-section of tablet P-11 showing Facies C over Facies A. Six-month intervals are indicated. (F) Optical microscope image of Facies C (mostly composed of calcite encrustations around algae (Al (tu)). Note the dense calcite-laminated structures made of calcified cyanobacterial filaments (Cy) that correspond to Facies A.

Fig. 3. Evolution of $\delta^{13}\text{C}$ and $\delta^{18}\text{O}$ values in tufa calcite, in the river water, and in the main springs of the Piedra River (Cimballa) from January 2010 to June 2012.

Fig. 4. Temporal evolution (2000-2012) of mean water $\delta^{18}\text{O}$ values in the Añamaza, Piedra and Ebrón Rivers.

Fig. 5. Downstream evolution of average water $\delta^{18}\text{O}$ values and $\delta^{13}\text{C}_{\text{DIC}}$ in the (A) Añamaza, (B) Piedra and (C) Ebrón Rivers.

Fig. 6. Average $\delta^{13}\text{C}$ (A, B, C) and $\delta^{18}\text{O}$ (D, E, F) (‰ V-PDB) values of tufa calcite from the Añamaza, Piedra and Ebrón Rivers. (A, D) the whole data set, (B, E) only facies A and (C, F) only facies C.

Fig. 7. Temporal evolution of $\delta^{18}\text{O}$ and $\delta^{13}\text{C}$ (‰ V-PDB) values of tufa calcite in facies A and C from the Añamaza, Piedra and Ebrón Rivers.

Fig. 8. Comparison between the temporal evolution of water temperature (T_w) estimated from $\delta^{18}\text{O}$ (‰ V-PDB) values in facies A and facies C, measured T_w (instantaneously and continuously recorded) and air temperature (T_{air}). The corresponding tendency lines are also displayed. (A) Añamaza River, (B) Piedra River and (C) Ebrón River. (D) Piedra River (Cool 2007-2008 - Cool 2009-2010).

Fig. 9. Comparison between the calculated fractionation coefficients in this paper and the defined in the literature. The actual fractionation coefficient of $\delta^{18}\text{O}$ is calculated

based on the measured $\delta^{18}\text{O}_{\text{calcite}}$ values and the average $\delta^{18}\text{O}_{\text{water}}$ values of warm and cool periods.

Fig. 10. Temporal evolution of average water $\delta^{18}\text{O}$, calcite $\delta^{18}\text{O}$ and $\delta^{13}\text{C}$, discharge of the water sampling month (June/January) and precipitation (2-month means for May and June/December and January). (A) Añamaza River, (B) Piedra River and (C) Ebrón River.

Table 1. Means of water temperature in cool and warm periods. Ranges and means of water $\delta^{13}\text{C}_{\text{DIC}}$ and $\delta^{18}\text{O}$ in the three rivers. In brackets, the periods in which the corresponding maxima and minima are recorded.

Table 2. Ranges and averages of calcite $\delta^{13}\text{C}_{\text{DIC}}$ and $\delta^{18}\text{O}$ in tufa calcite during warm and cool periods in the three studied rivers.

Figure and table captions of the Appendix

Fig. A1 Temporal evolutions of the water temperatures recorded in the three rivers.

Fig. A2. Mean values of $\delta^{13}\text{C}_{\text{DIC}}$ V-PDB (A) and $\delta^{18}\text{O}$ V-SMOW (B) in the river waters of the Añamaza, Piedra and Ebrón Rivers. Data partially taken from Osácar et al. 2013a, Auqué et al., 2014 and Arenas et al., 2015.

Fig. A3. $\delta^{13}\text{C}$ and $\delta^{18}\text{O}$ (‰ V-PDB) values of calcite samples analysed from deposits on tablets. Long records (P-14, 16, 20, 11 and 12) correspond to successive tablets installed at the same sites. Note that two to three samples were analysed in some intervals. Gaps

within the series are due to the lack of a corresponding sediment record caused by erosion.

Table A1. Summarized information from the studied valleys (climate, hydrology and drainage area from Sancho et al., 2015), and hydrochemical parameters (this paper and Auqué et al., 2014, Osácar et al., 2013a, and Arenas et al., 2015). Annual discharge data are available from <http://www.chebro.es> (Añamaza and Piedra rivers) and <http://www.chj.es> (Ebrón River).

Table A2. Data of tufa calcite $\delta^{13}\text{C}$ and $\delta^{18}\text{O}$ (‰VPDB), river water $\delta^{18}\text{O}$ (‰VSMOW) and $\delta^{13}\text{C}_{\text{DIC}}$ (‰VPDB), and water T measured during sampling. Water data partially taken from Osácar et al. 2013a, Auqué et al., 2014 and Arenas et al., 2015.

Table A3. Calculated water temperatures from tufa calcite $\delta^{18}\text{O}$ in the three studied rivers

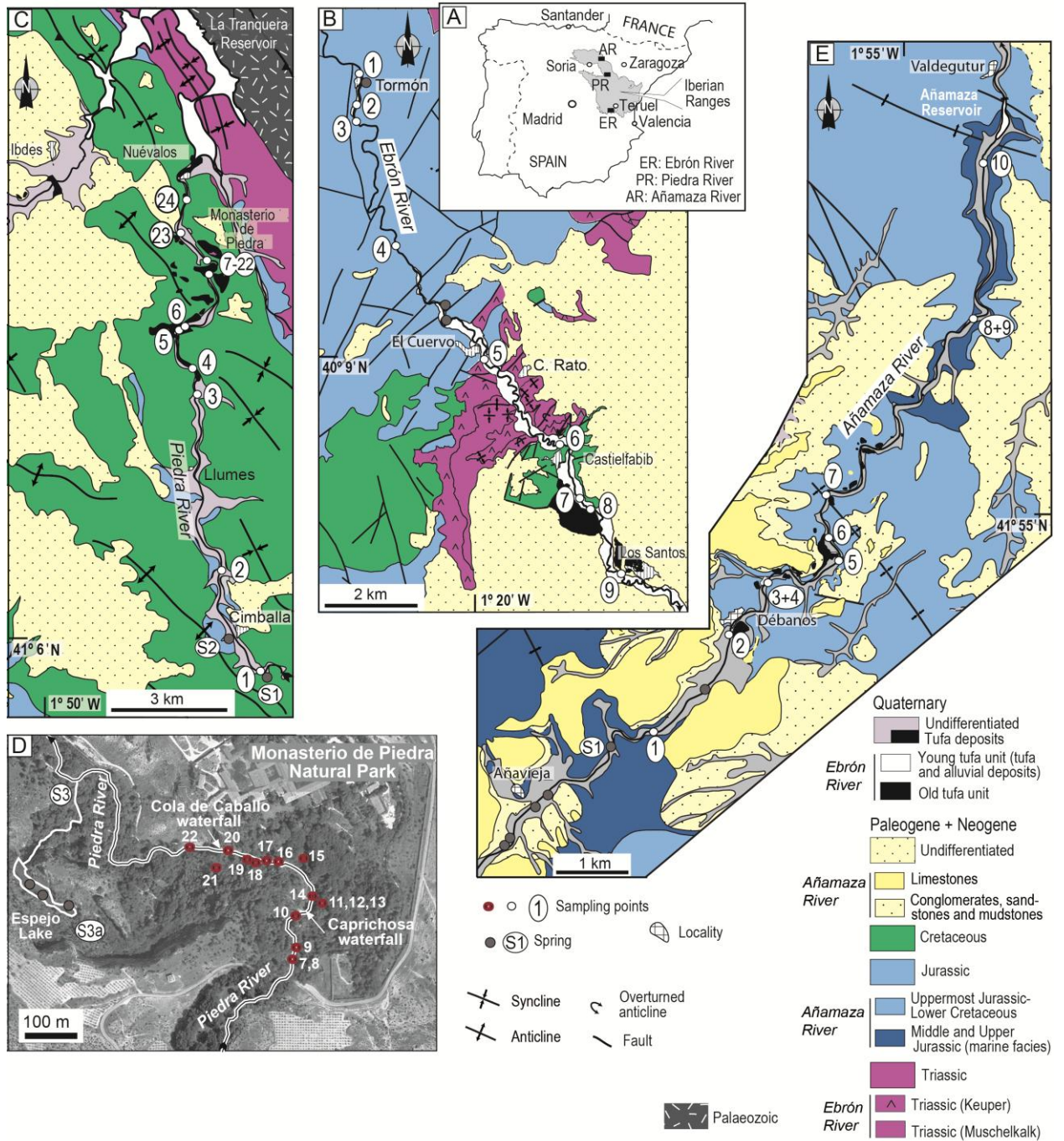


Figure 1

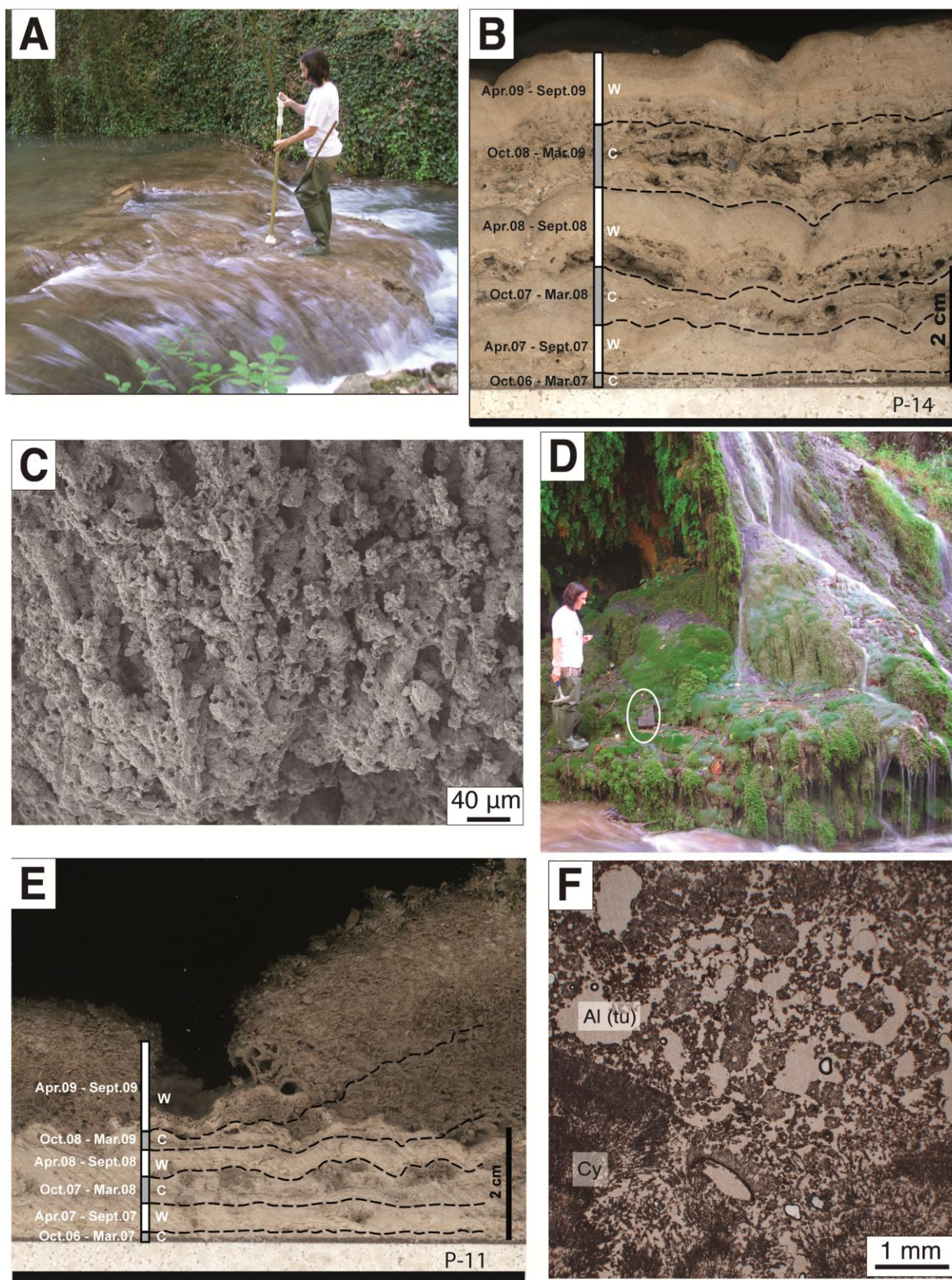


Figure 2

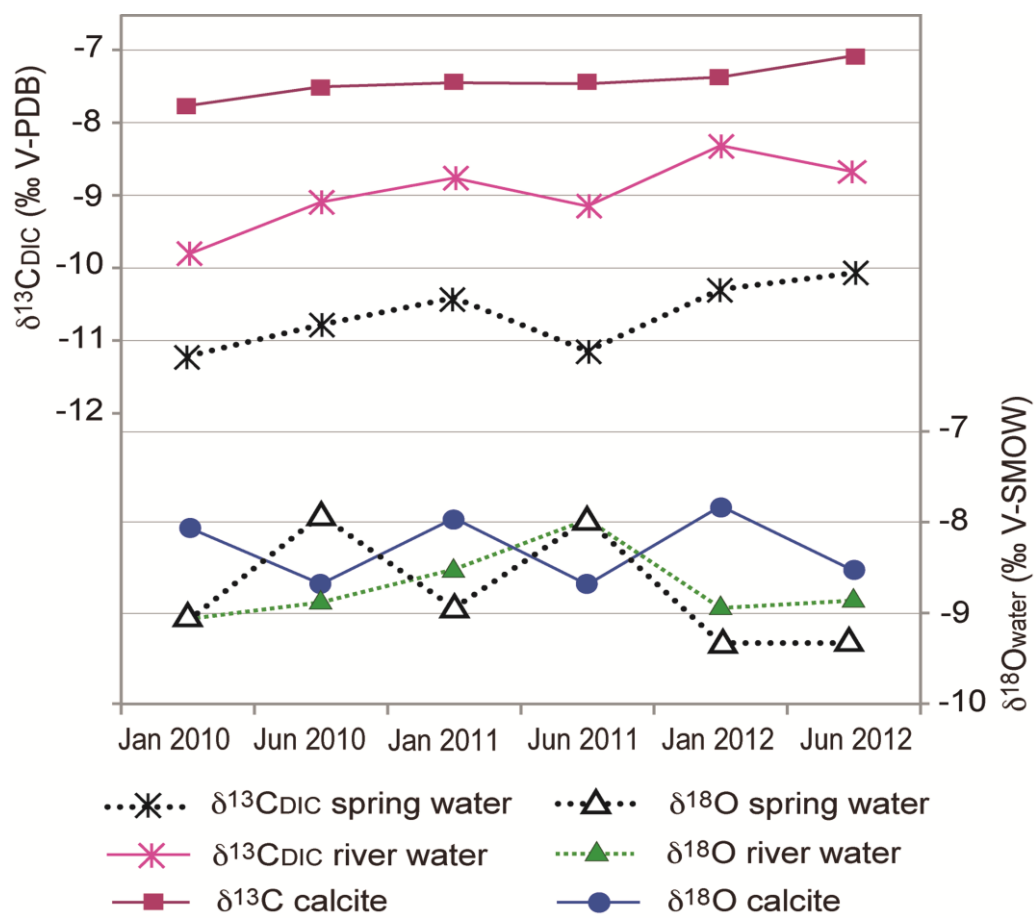


Figure 3

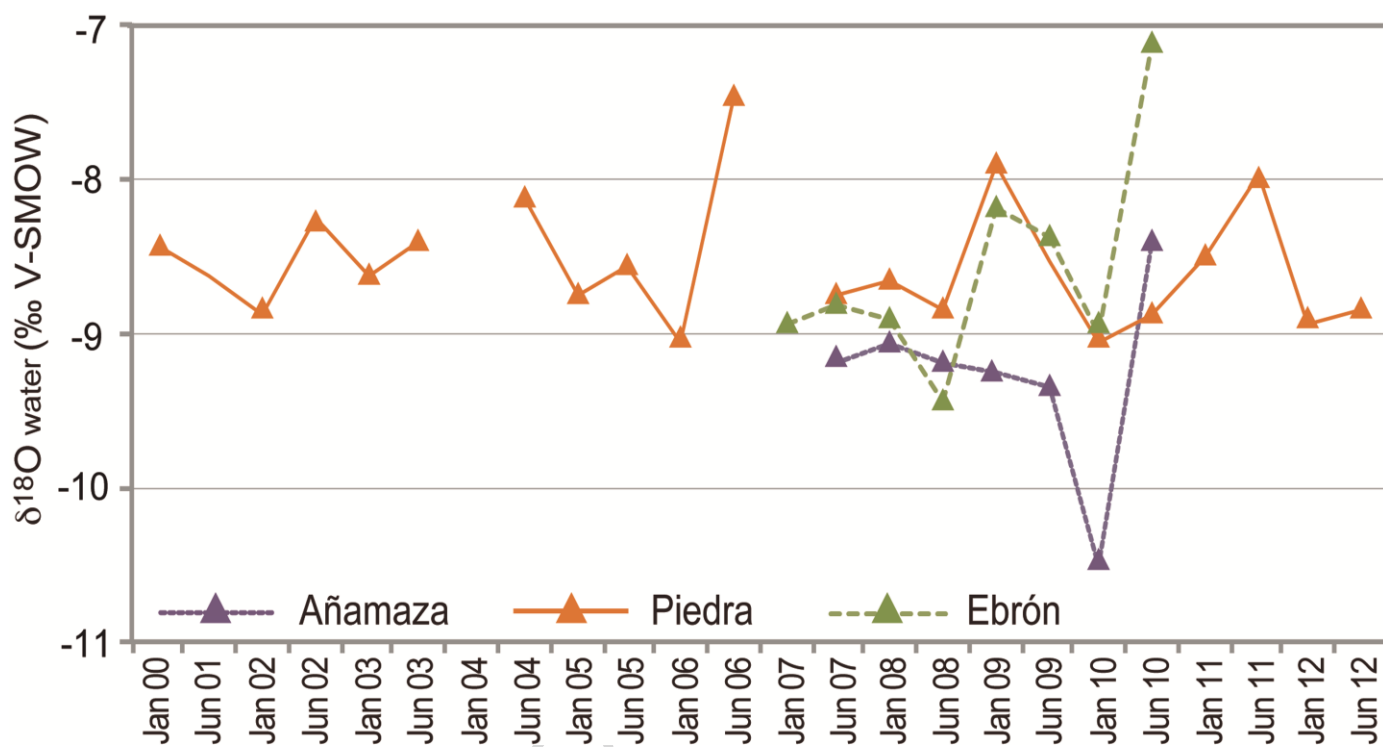


Figure 4

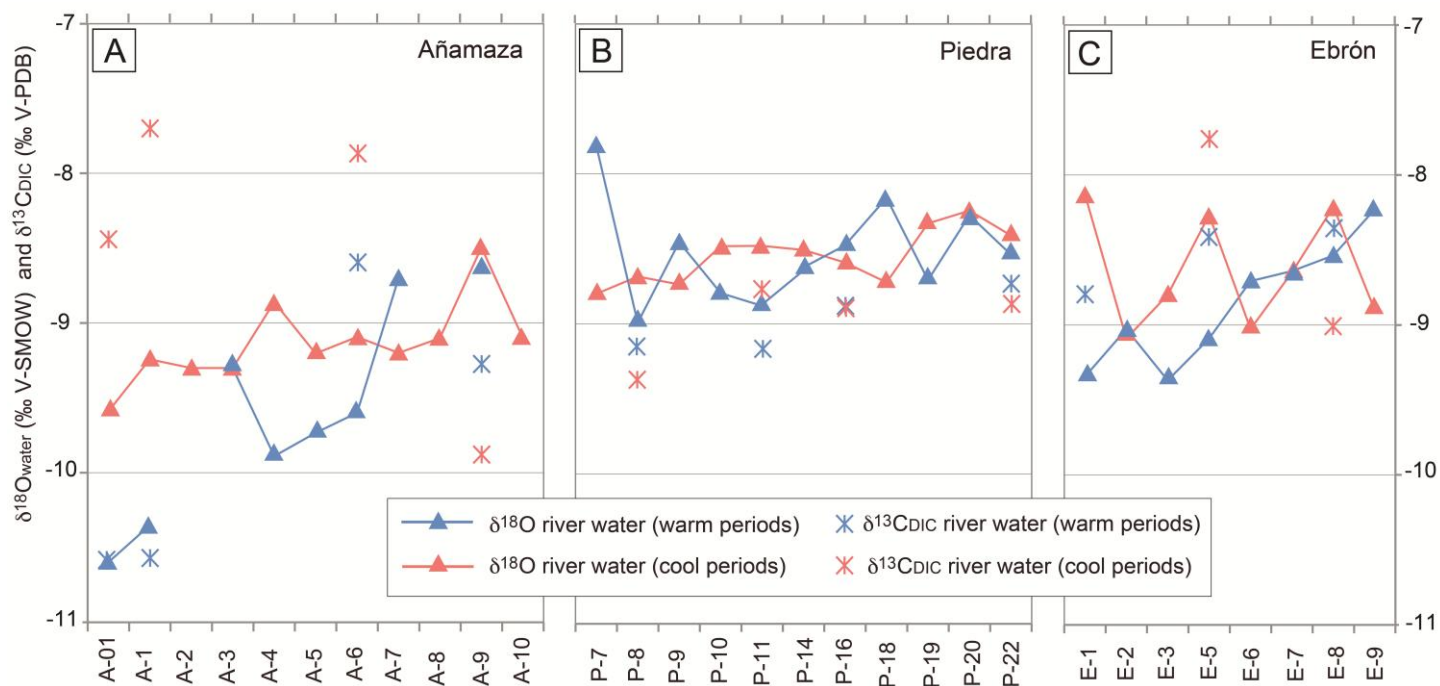


Figure 5

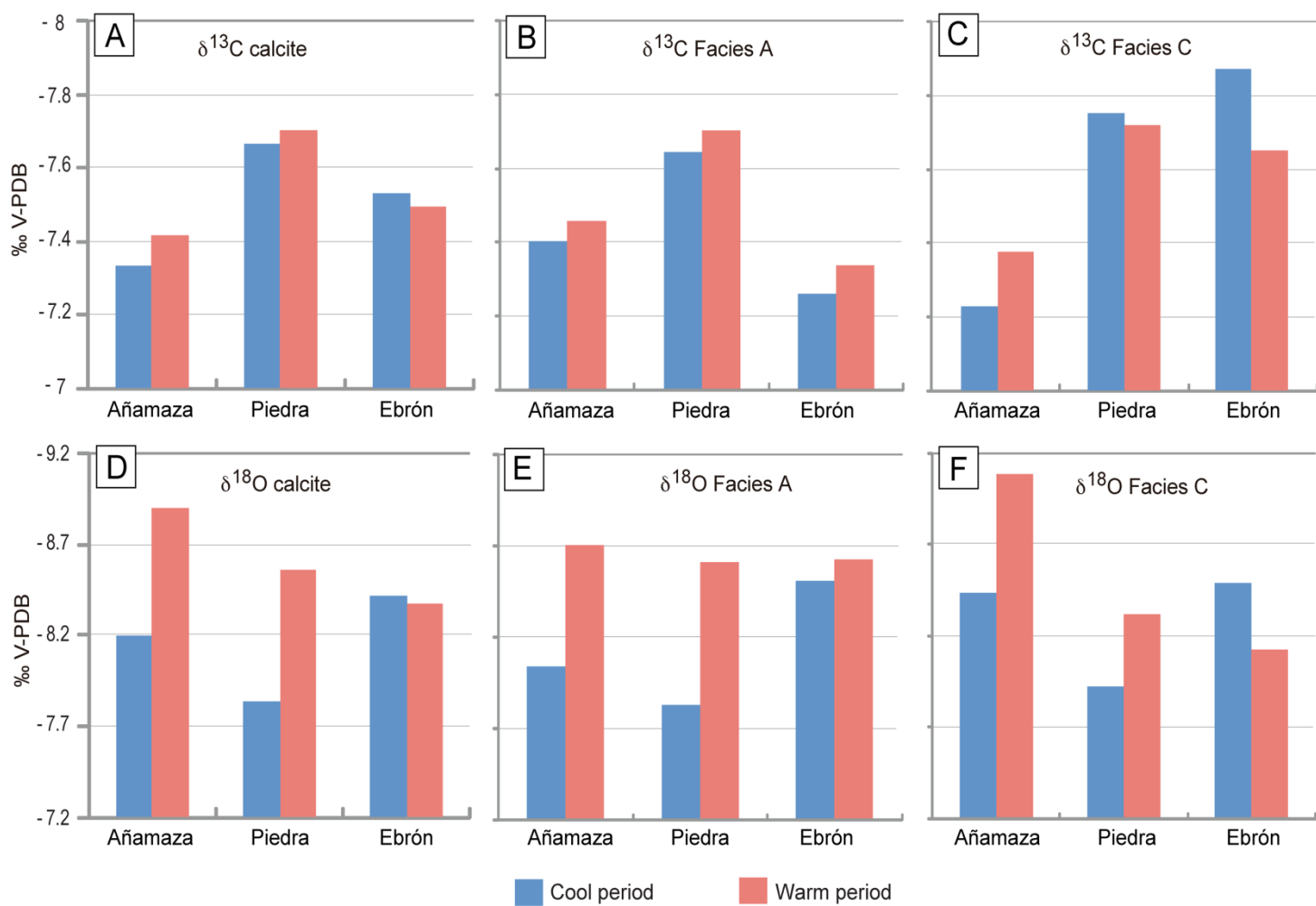


Figure 6

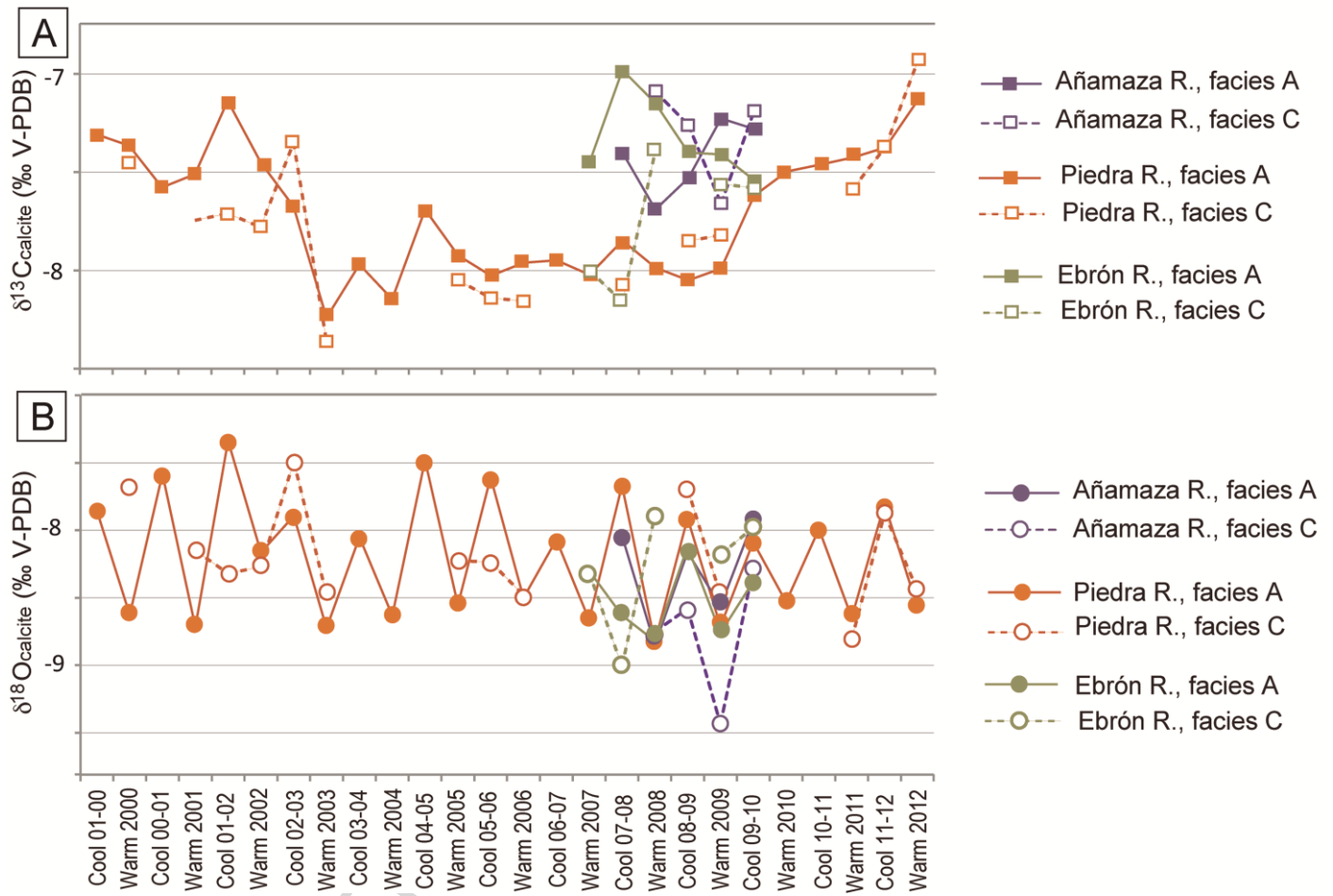


Figure 7

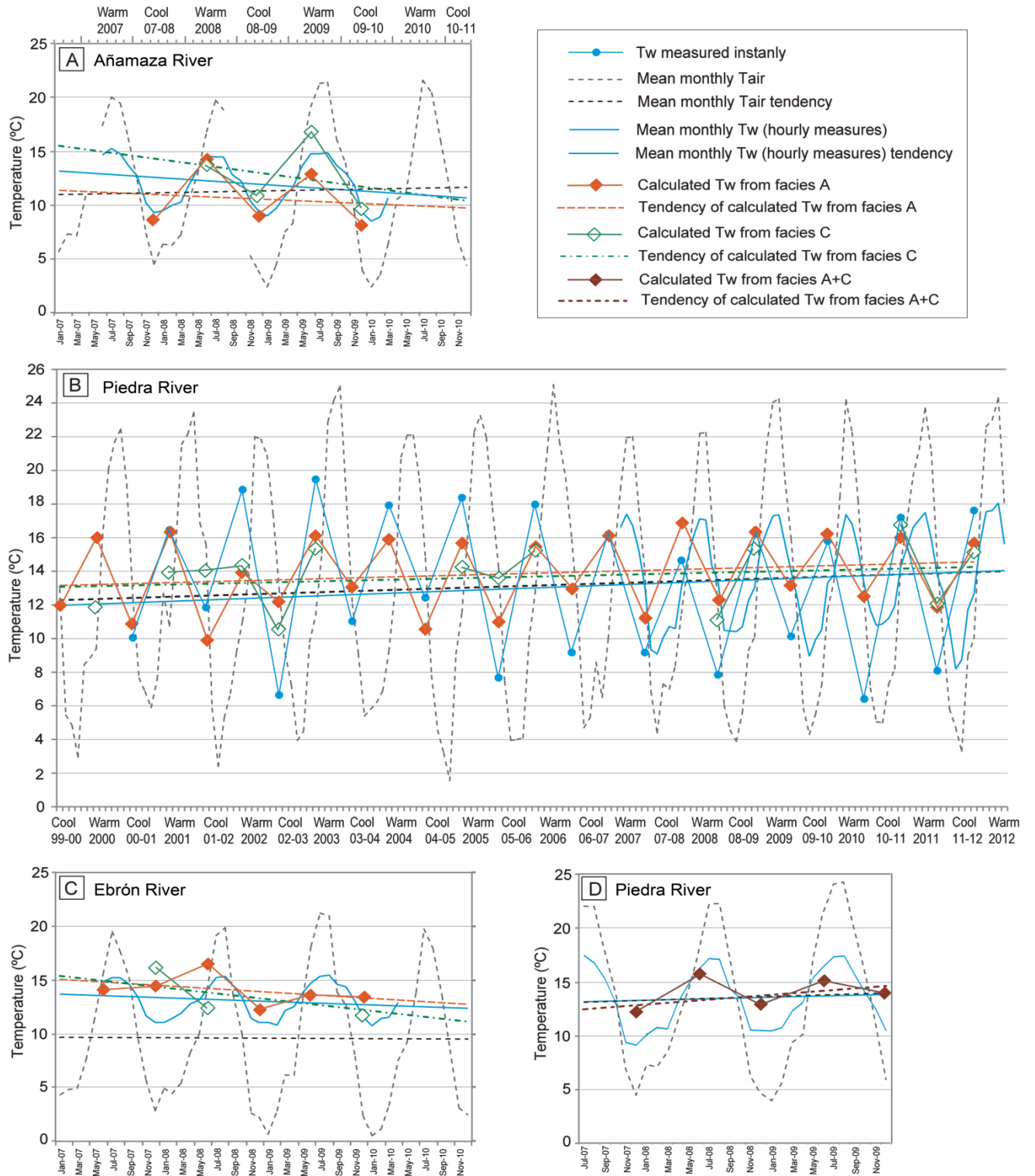


Figure 8

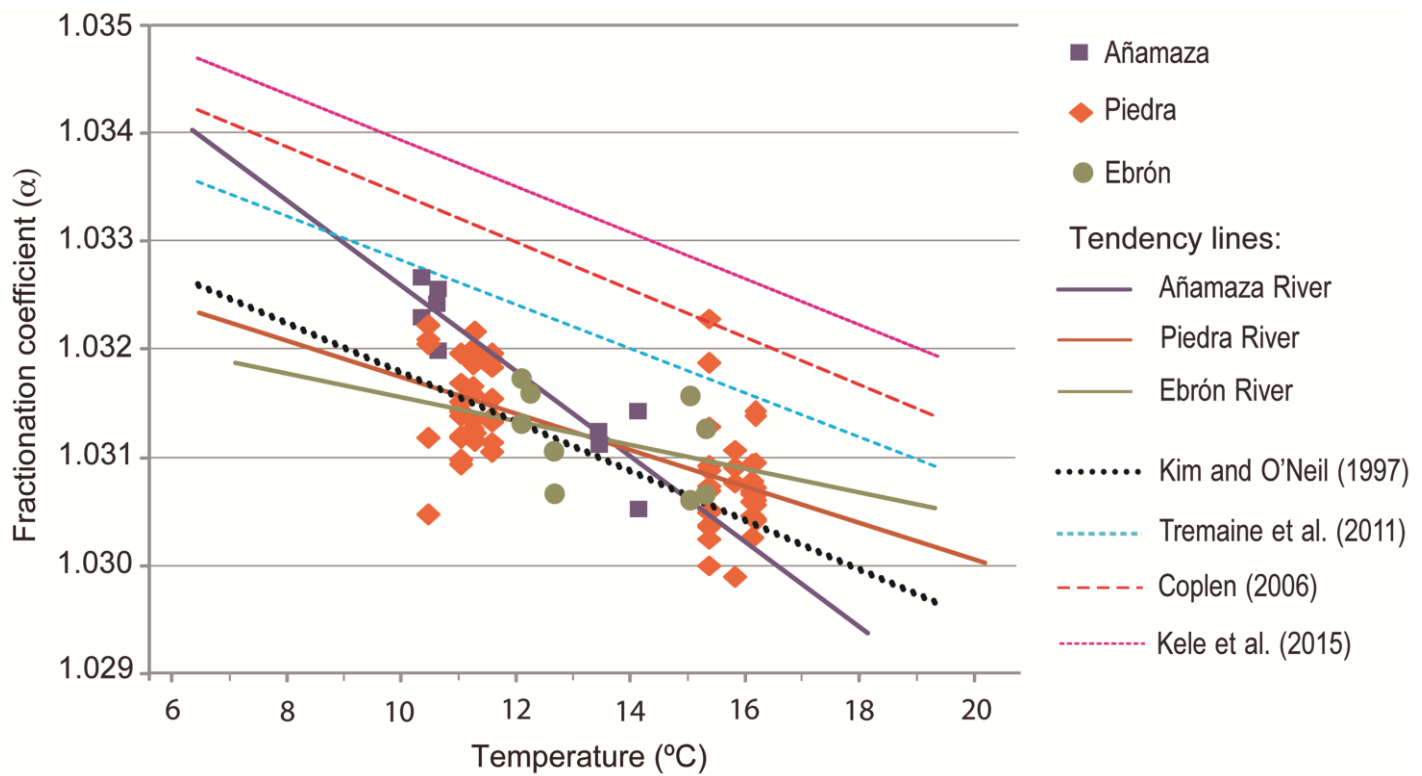


Figure 9

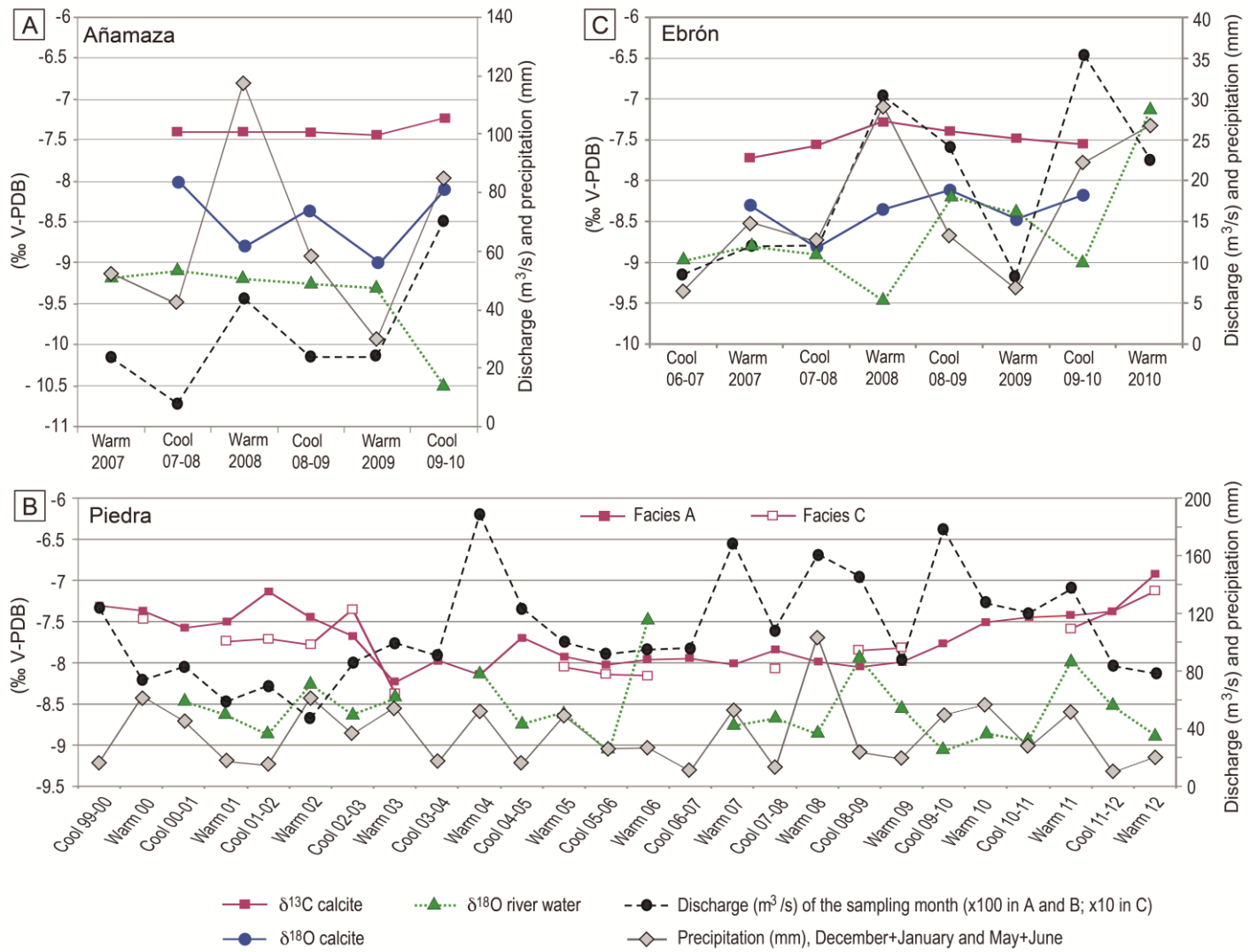


Figure 10

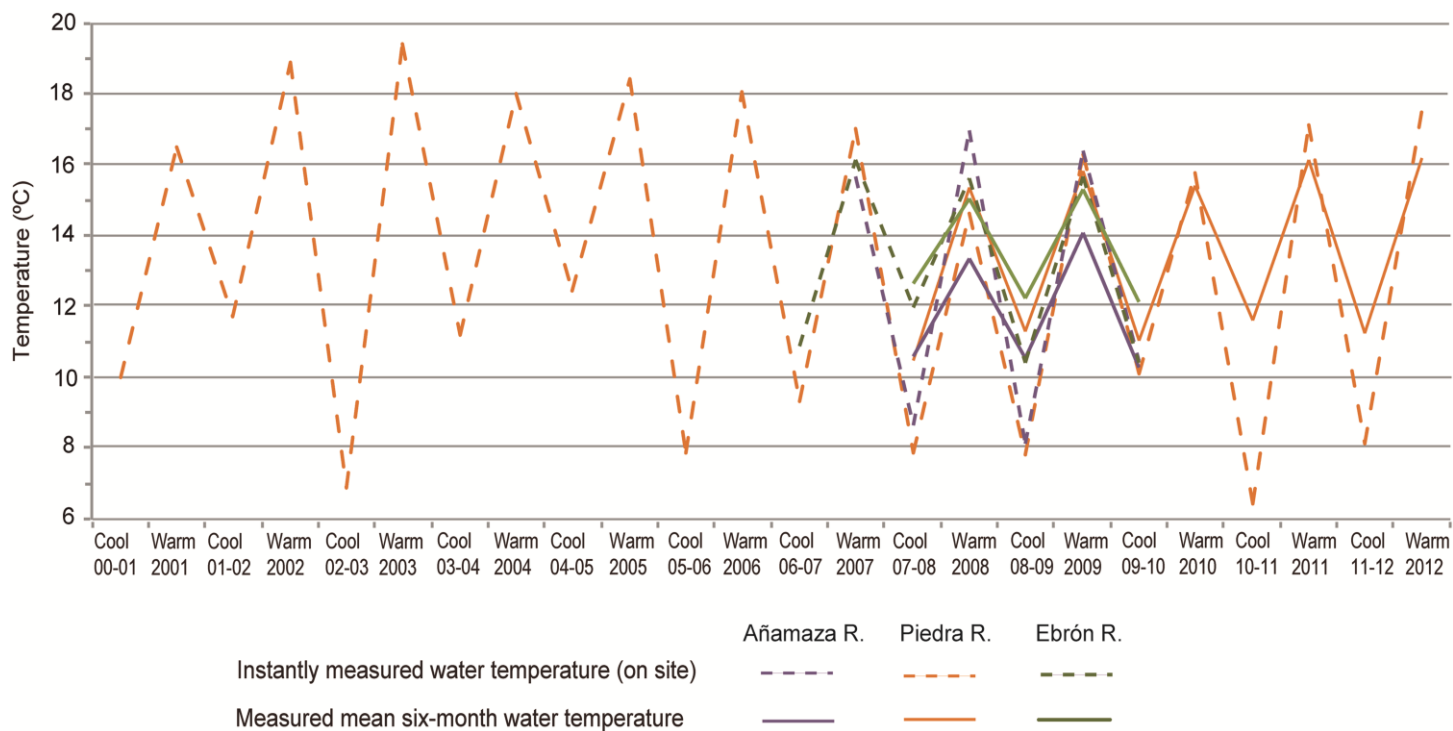


Figure A1

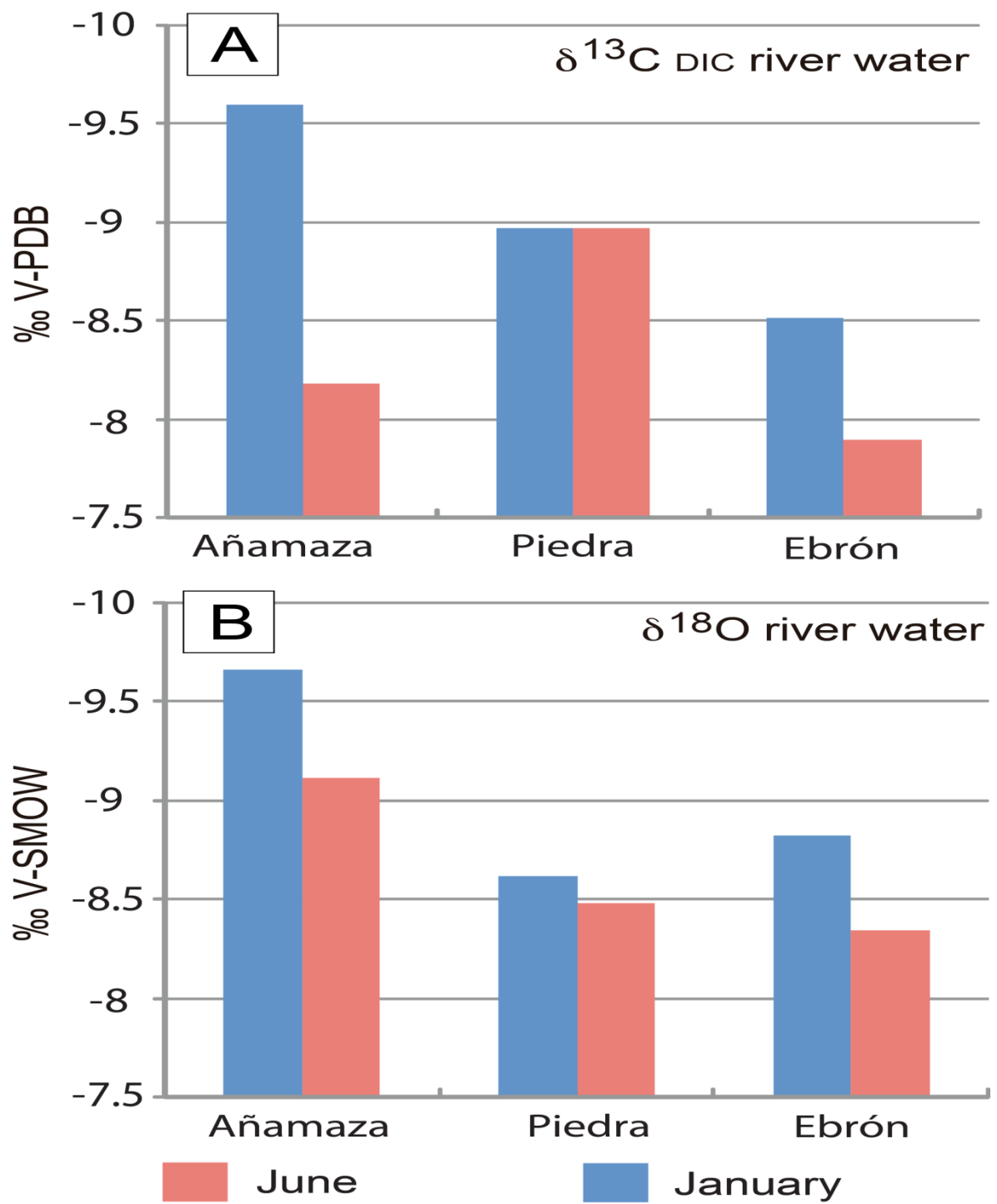


Figure A2

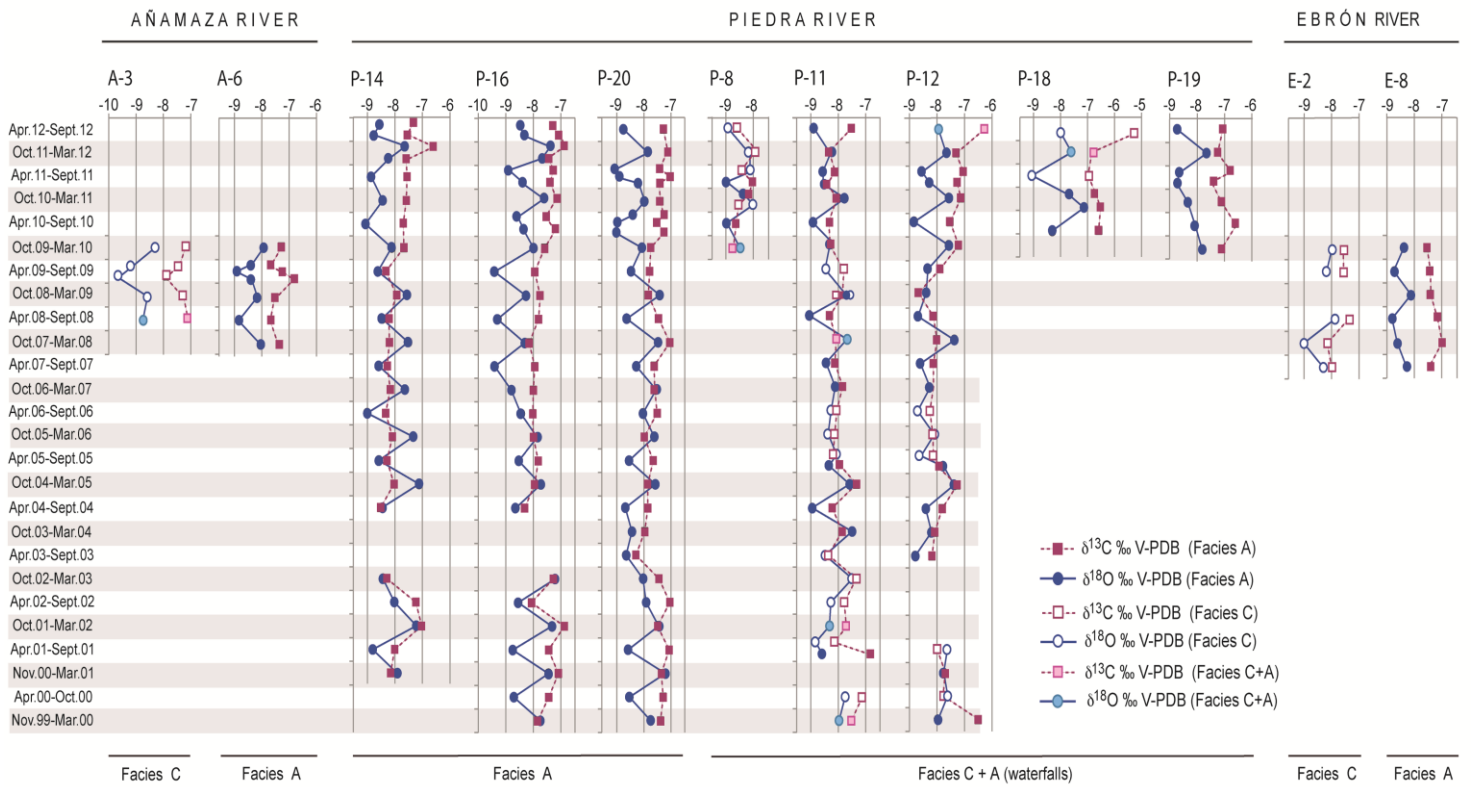


Figure A3

	Temperature °C				Water $\delta^{13}\text{C}_{\text{DIC}}$ ‰ VPDB				Water $\delta^{18}\text{O}$ ‰ VSMOW			
	Mean instantaneous temperature		Mean sensor temperature		Maximum	Minimum	Mean June	Mean January	Maximum	Minimum	Mean January	Mean June
	warm	cool	warm	cool								
Añamaza River	16.3	9.1	13.6	10.4	-7.0 (June 2010)	-10.6 (January 2010)	-8.2	-9.6	-8.7 (January 2008)	-10.9 (January 2010)	-9.7	-9.1
Piedra River	17.3	9.1	15.5	10.9	-8.1 (January 2012)	-10.5 (January 2010)	-9.0	-9.0	-7.3 (June 2006)	-9.6 (January 2010)	-8.6	-8.5
Ebrón River	15.8	10.9	14.3	11.8	-6.9 (June 2010)	-9.0 (June 2010)	-7.9	-8.5	-7.9 (January 2009)	-9.9 (Warm 2008)	-8.8	-8.6

Table 1. Means of water temperature in cool and warm periods. Ranges and means of water $\delta^{13}\text{C}_{\text{DIC}}$ and $\delta^{18}\text{O}$ in the three rivers. In brackets, the periods in which the corresponding maxima and minima are recorded.

	$\delta^{13}\text{C}\text{‰PDB}$				$\delta^{18}\text{O}\text{‰PDB}$			
	Maximum	Minimum	Mean Warm periods	Mean Cool periods	Maximum	Minimum	Mean Warm periods	Mean Cool periods
Añamaza River	-6.79 (Warm 2009)	-7.95 (Cool 2008-2009)	-7.42	-7.33	-7.93 (Cool 2009-2010)	-9.66 (Warm 2009)	-8.90	-8.20
Piedra River	-5.28 (Warm 2012)	-8.75 (Cool 2009-2010)	-7.70	-7.66	-7.12 (Cool 2010-2011)	-9.41 (Warm 2009)	-8.56	-7.84
Ebrón River	-6.98 (Cool 2007-2008)	-8.16 (Cool 2007-2008)	-7.49	-7.53	-7.89 (Warm 2008)	-9.01 (Cool 2007-2008)	-8.38	-8.42

Table 2. Ranges and averages of calcite $\delta^{13}\text{C}_{\text{DIC}}$ and $\delta^{18}\text{O}$ in tufa calcite during warm and cool periods in the three studied rivers. In brackets, the periods in which the corresponding maxima and minima are recorded.

River	Mean annual temperature (°C)	Annual precipitation (mm/yr)	Mean yearly discharge of the river (m ³ /s)	Length of the studied river stretch (km)	altitude of the studied river stretch (m)	Geological bedrock of catchment basin	Conductivity $\mu\text{S cm}^{-1}$	SO ₄ mg/L	Ca mg/L	Alkalinity mg/L	Log pCO ₂	SIc
Añamaza	11.1	564	0.16	18	1013 - 561	Jurassic limestones and marls Cretaceous sandstones and mudstones Tertiary conglomerates, sandstones and limestones	786	220	132	248	-2.11	+1.37
Piedra	14	397.4	1.06	0.4	786	Lower Cretaceous sandstones Upper Cretaceous limestones and dolostones Tertiary conglomerates, sandstones and mudstones	634	106	87.7	270	-2.79	+0.79
Ebrón	10.8	450	1.2	22	1050 - 740	Jurassic limestones Cretaceous sandstones and dolostones Tertiary conglomerates, sandstones and mudstones	528	80	84.2	266	-2.44	+1.0

Table A1. Summarized information from the studied valleys (climate, hydrology and drainage area from Sancho et al., 2015), and hydrochemical parameters (this paper and Auqué et al., 2014, Osácar et al., 2013a, and Arenas et al., 2015). Annual discharge data are available from <http://www.chebro.es> (Añamaza and Piedra rivers) and <http://www.chj.es> (Ebrón River).

Sites	Sediment $\delta^{13}\text{C}$ (‰ VPDB)	Sediment $\delta^{18}\text{O}$ (‰ VPDB)	Water $\delta^{18}\text{O}$ (‰ VSMOW)	Water $\delta^{13}\text{CDIC}$ (‰ VPDB)	Water T (°C)
<i>Cool 1999-2000</i>					
P-11	-7.52	-7.97			
P-12	-6.48	-7.96			
P-16	-7.84	-7.74			
P-20	-7.39	-7.75			
<i>Cool 2000-2001</i>					
P-10			-8.6		10.7
P-11					
P-12	-7.70	-7.75	-8.6		9.7
P-14	-8.16	-7.92			
P-16	-7.09	-7.45	-7.9		10.4
P-19			-8.6		10.5
P-20	-7.36	-7.21			
P-22			-8.6		8.6
<i>Cool 2001-2002</i>					
P-10			-9.08		12.2
P-11	-7.71	-8.32	-8.83		12
P-14	-7.03	-7.22			
P-16	-6.88	-7.33	-8.94		12.2
P-18					12
P-19			-8.87		11.9
P-20	-7.50	-7.46			
P-22			-8.65		11.7
<i>Cool 2002-2003</i>					
P-8					
P-10			-8.6		8.1
P-11	-7.35	-7.49	-8.7		6.6
<i>Warm 2000</i>					
P-11	-7.12	-7.75			
P-12	-7.78	-7.61			
P-16	-7.44	-8.71			
P-20	-7.29	-8.54			
<i>Warm 2001</i>					
P-10			-8.78		16.9
P-11a	-6.8	-8.54	-8.67		16.4
P-11b	-8.18	-8.82			
P-12	-8.00	-7.62			
P-14	-8.01	-8.81			
P-16	-7.45	-8.75	-8.57		16.5
P-19			-8.33		16.6
P-20	-7.07	-8.59			
P-22			-8.76		16.2
<i>Warm 2002</i>					
P-10			-8.31		18.8
P-11	-7.78	-8.27	-8.09		18.8
P-14	-7.24	-8.02			
P-16	-8.07	-8.55	-8.08		18.9
P-18					
P-19			-8.43		18.5
P-20	-7.04	-7.92			
P-22			-8.33		19.4
<i>Warm 2003</i>					
P-8					19.1
P-10			55 -8.6		19.2
P-11	-8.36	-8.48	-8.2		19.4

P-14	-8.30	-8.44			P-12	-8.18	-8.79		
P-16	-7.28	-7.21	-8.5	6.7	P-14			-8.4	19.4
P-19			-8.7		P-16				19.4
P-20				6.4	P-19			-8.1	19.5
					P-20	-8.30	-8.66	-8.2	19.6
P-22		-8.7		6.6	P-22			-9.0	19.6
<hr/>					<hr/>				
<i>Cool 2003-2004</i>					<i>Warm 2004</i>				
P-8				12.2	P-8				18.1
P-10					P-10			-8.43	18.0
P-11	-7.86	-7.50		11.50	P-11	-8.22	-8.95	-8.03	17.8
P-12	-8.08	-8.20		10.90	P-12	-7.81	-8.41		
P-14					P-14	-8.52	-8.52	-8.23	17.8
					P-16	-8.32	-8.64		18.0
P-19				11.20	P-19			-8.27	18.4
P-20	-7.97	-8.45		11.00	P-20	-7.86	-8.69	-8	18.1
P-22				10.8	P-22			-7.82	17.8
<hr/>					<hr/>				
<i>Cool 2004-2005</i>					<i>Warm 2005</i>				
P-8				13.1	P-8				18.2
P-10			-8.83	12.8	P-10			-8.75	18.2
P-11	-7.34	-7.59	-9.01	12.7	P-11a	-7.93	-8.34	-8.75	18.3
					P-11b	-8.19	-8.15		
P-12	-7.27	-7.38			P-12a	-7.95	-7.78		
					P-12b	-8.13	-8.63		
P-14	-8.03	-7.12	-8.9	12.4	P-14	-8.29	-8.58	-8.7	18.4
P-16	-7.95	-7.73		12.3	P-16	-7.82	-8.53		18.4
P-19			-8.71	11.7	P-19				18.5
P-20	-7.86	-7.58	-8.19	12.3	P-20	-7.66	-8.55	-8.61	18.4
P-22			-8.88	12.1	P-22				19.2
<hr/>					<hr/>				
<i>Cool 2005-2006</i>					<i>Warm 2006</i>				
P-7					P-7				
P-8				8.8	P-8				18.3
P-9					P-9				

P-10			-9.48	8.3	P-10			-8.49	18.2
P-11	-8.13	-8.37	-9.28	7.5	P-11	-8.05	-8.26	-7.58	18.2
P-12	-8.15	-8.10			P-12	-8.26	-8.70		
P-14	-8.09	-7.34	-8.99	7.9	P-14	-8.34	-9.01	-7.58	17.9
P-16	-8.00	-7.86		7.5	P-16	-8.02	-8.45		17.9
P-19			-9.2	7.4	P-19			-7.29	18.3
P-20	-7.99	-7.62	-8.39	7.8	P-20	-7.52	-8.04	-7.37	17.9
P-22			-9.05	7.6	P-22			-7.56	17.6
<i>Cool 2006-2007</i>					<i>Warm 2007</i>				
A-1			-9.2		A-1			-9.2	15.3
A-2			-9.3		A-2			-9.3	15.8
A-3			-9.3		A-3			-9.3	15.7
A-4					A-4				
A-5			-9.1		A-5			-9.1	16.1
A-6			-9.2		A-6			-9.2	15.6
A-7			-9.2		A-7			-9.2	15.8
A-8			-9.1		A-8			-9.1	15.4
P-7				9.7	P-7			-8.8	19.4
P-8				9.7	P-8			-8.9	19.4
P-9				9.7	P-9			-8.8	19.4
P-10				9.8	P-10			-8.7	16.2
P-11	-7.84	-8.11		9.2	P-11	-8.12	-8.44	-8.7	16.1
P-12	-8.13	-8.25		9.2	P-12	-8.13	-8.60	-8.8	16.1
P-14	-8.17	-7.64		9.0	P-14	-8.28	-8.59	-8.6	16.1
P-16	-8.00	-8.80		9.2	P-16	-7.95	-9.40	-8.7	16.2
P-18				8.3	P-17			-8.8	
P-19				9.2	P-18			-8.8	16.2
P-20	-7.60	-7.55		9.3	P-19				16.5
P-22				9.5	P-20	-7.63	-8.29	-8.9	16.4
					P-22			-8.7	16.3
E-1			-9.31	11.8	E-1			-8.7	15.7

E-2		-9.08		11.1	E-2	-8	-8.31	-8.8	15.1
E-3		-9.37		11.7	E-3			-8.8	15.6
E-5		-8.99		13	E-5			-8.8	17.7
E-6		-8.96		10.5	E-6			-8.8	17
E-7		-9.3		8.9	E-7			-8.8	16.2
E-8		-8.41		10.1	E-8	-7.45	-8.3	-8.9	16
E-9		-8.23		10.1	E-9			-8.9	15.8
<hr/>					<hr/>				
<i>Cool 2007-2008</i>					<i>Warm 2008</i>				
A-1					A-1			-9.2	17
A-2					A-2			-9.3	
A-3		-9.3		9.4	A-3	-7.09	-8.75	-9.3	17.2
A-4		-9.2		8	A-4				
A-5		-9.3		8.4	A-5			-9.1	17.3
A-6	-7.4	-8.04	-8.9	8.5	A-6	-7.69	-8.85	-9.2	17.6
A-7			-8.7	8.5	A-7			-9.2	
A-8					A-8			-9.1	
A-9			-9.1	9.1	A-9				
A-10					A-10			-9.1	15.8
<hr/>					<hr/>				
P-7				9.7	P-7				14.4
P-8					P-8				14.4
P-9			-8.7	9.8	P-9			-9.16	14.3
P-10			-8.7	9.8	P-10			-9.04	14.4
P-11	-8.07	-7.67	-8.7	9.2	P-11	-8.31	-9.04	-8.84	14.4
P-12	-8.00	-7.36			P-12	-8.13	-8.69		
P-14	-8.20	-7.52	-8.6	9.0	P-14	-8.22	-8.47	-8.74	14.5
P-16	-8.15	-8.31	-8.8	9.2	P-16	-7.81	-9.30	-9.02	14.5
P-18			-8.5	8.3	P-18			-8.76	14.6
P-19			-8.7	9.2	P-19			-8.66	14.8
P-20	-7.04	-7.48	-8.7	9.3	P-20	-7.46	-8.64	-8.91	15.2
P-22			-8.6	9.5	P-22			-8.64	15.3
<hr/>					<hr/>				
E-1				10.7	E-1				15.5

E-2	-8.16	-9.01	-8.9	10.6	E-2	-7.39	-7.89	-9.85	14.7
E-3				11.6	E-3				15.4
E-5				13.2	E-5				16.7
E-6			-8.9	12.6	E-6			-9.92	16
E-7			-8.9	12.2	E-7			-8.83	16
E-8	-6.98	-8.63	-8.9	12.2	E-8	-7.15	-8.82	-9.24	15.5
E-9				12.9	E-9				15
<hr/> <i>Cool 2008-2009</i>					<hr/> <i>Warm 2009</i>				
A-01					A-01			-9.59	16.4
A-1					A-1			-9.75	16.8
A-2					A-2				
A-3	-7.26	-8.58			A-3a	-7.46	-9.21		
					A-3b	-7.86	-9.66		
A-4			-9.56	7.6	A-4			-9.45	16.9
A-5			-9.47	8.9	A-5			-9.41	16.7
A-6a	-7.95	-8.6	-9.15	8.5	A-6a	-7.65	-8.41	-9.33	16.2
A-6b	-7.53	-8.16			A-6b	-7.24	-8.9		
					A-6c	-6.79	-8.38		
A-7					A-7				
A-8					A-8				
A-9			-8.84	7.5	A-9			-9.08	15.3
A-10					A-10				
<hr/>					<hr/>				
P-7			-7.81	8.5					
P-8			-8.13		P-8				
P-9			-8.21	8.2	P-9			-8.25	16.2
P-10			-8.25	8.4	P-10			-8.29	16.4
P-11a	-8.07	-7.56		7.4	P-11	-7.82	-8.48	-8.75	15.9
P-11b	-7.85	-7.69							
P-12	-8.67	-8.39			P-12	-7.89	-8.33		
P-14	-7.94	-7.56	-8	8.0	P-14	-8.33	-8.62	-9.32	16.2
P-16	-7.75	-8.27	-7.75	7.9	P-16	-7.95	-9.41	-8.96	16.3
P-18			-7.82	6.3	P-18			-8.61	15.9

P-19			-8.22		7.5	P-19			-8.51		16.6
P-20	-7.84	-7.42	-7.82		8.1	P-20	-7.79	-8.48	-8.12		16.8
P-22			-7.3		7.8	P-22			-8.13		16.3
<hr/>						<hr/>					
E-1					9	E-1			-8.52		15.3
E-2			-8.59		9.9	E-2	-7.56	-8.18	-8.62		15
E-3					10.1	E-3					14.9
E-5					11.3	E-5			-8.47		16.3
E-6			-8.25		10.8	E-6			-8.36		16.3
E-7			-7.94		10.5	E-7			-8.32		16.1
E-8	-7.4	-8.12	-7.97		10.7	E-8	-7.41	-8.76	-7.98		15.6
E-9					11	E-9					15.7
<hr/>						<hr/>					
<i>Cool 2009-2010</i>						<i>Warm 2010</i>					
A-01			-10.6	-10.60	10	A-01			-8.44		
A-1			-10.57	-10.35	10.3	A-1			-8.82	-7.71	
A-2						A-2					
A-3	-7.19	-8.29				A-3					
A-4			-10.91	-9.84	10.6	A-4			-8.27	-6.98	
A-5			-10.43		10.9	A-5					
A-6	-7.28	-7.93	-10.75	-8.58	10.4	A-6			-8.64	-7.87	
A-7						A-7					
A-8						A-8					
A-9			-9.88	-9.88	10.5	A-9			-7.91	-9.88	
A-10						A-10					
<hr/>						<hr/>					
P-8	-8.75	-8.51	-9.58	-9.7	10.3	P-8	-8.64	-8.96	-8.77	-9.46	15.5
P-10					10.1	P-10					15.7
P-11	-7.67	-8.12	-9.2	-10.5	10.0	P-11	-7.70	-9.07	-8.94	-8.90	15.6
P-12	-7.21	-7.56				P-12	-7.52	-8.83			
P-14	-7.67	-8.12			10.1	P-14	-7.70	-9.07			15.6
P-16	-7.59	-7.99	-8.94	-9.6	10.1	P-16a	-7.18	-8.35	-8.8	-8.93	15.7
						P-16b	-7.50	-8.56			
						P-18	-6.59	-8.30			16.0

P-19	-7.11	-7.82			10.0	P-19	-6.57	-8.07			16.1
P-20	-7.75	-8.08			10.2	P-20a	-7.26	-9.03			16.0
						P-20b	-7.51	-8.98			
						P-20c	-7.26	-8.41			
P-22	-7.17	-8.55	-8.54	-9.5	10.2	P-22			-9.02	-9.09	15.9
<hr/>						<hr/>					
E-1			-9.38	-8.80	9.3	E-1			-7.17	-6.91	
E-2	-7.58	-7.98			9.6						
E-3					9.8	E-3					
E-5				-8.40	11.4	E-5			-7.53	-7.76	
E-6					11.1	E-6					
E-7			-8.42		10.8	E-7					
E-8	-7.54	-8.38	-8.87	-8.35	10.8				-6.73	-9.01	
E-9					10.6	E-9					
<hr/>						<hr/>					
<i>Cool 2010-2011</i>						<i>Warm 2011</i>					
P-8a	-8.13	-8.33	-8.9	-9.18	5.9	P-8a	-8.39	-8.09	-8.28	-9.61	16.7
P-8b	-8.56	-8.01				P-8b	-7.99	-9.03			
P-10					6.6	P-10					16.8
P-11	-7.59	-8.44	-8.52	-8.60	5.4	P-11	-7.56	-8.86	-8.22	-8.95	17.2
P-12	-7.13	-7.56				P-12a	-7.25	-8.27			
						P-12b	-7.03	-8.54			
P-14	-7.59	-8.44			6.6	P-14	-7.56	-8.86			17.1
P-16	-7.16	-7.62	-8.23	-8.68	6.4	P-16a	-7.39	-8.39	-7.83	-9.05	17.6
						P-16b	-7.28	-8.88			
P-18a	-6.72	-7.68				P-18	-6.98	-9.06			
P-18b	-6.52	-7.11				P-19a	-6.76	-8.63			17.6
P-19	-7.12	-8.35			6.9	P-19b	-7.47	-8.72			
P-20	-7.40	-7.97			7.1	P-20a	-7.41	-8.21			17.3
						P-20b	-7.04	-8.92			
						P-20c	-7.42	-9.09			
P-22			-8.42	-8.59	6.6	P-22			-7.55	-8.99	16.9
<hr/>						<hr/>					
<i>Cool 2011-2012</i>						<i>Warm 2012</i>					
P-8	-7.90	-8.16	-9.36	-8.61	8.5	P-8	-8.57	-8.91	-8.79	-9.04	17.1

P-10					8.5	P-10					17.1
P-11a	-7.59	-8.24	-9.05	-8.41	7.6	P-11a	-7.59	-8.80	-8.93	-8.46	17.7
P-11b	-6.59	-7.61				P-11b	-7.33	-8.57			
P-12	-7.31	-7.66				P-12	-6.30	-7.94			
P-14a	-7.59	-8.24				P-14a	-7.59	-8.80			17.5
P-14b	-6.59	-7.61			8.5	P-14b	-7.33	-8.57			
P-16a	-7.43	-7.67	-8.75	-8.26	8.1	P-16a	-7.07	-8.31	-8.76	-8.69	17.7
P-16b	-6.88	-7.37				P-16b	-7.26	-8.46			
P-18	-6.84	-7.59			7.6	P-18	-5.28	-7.98			17.6
P-19	-7.25	-7.65			8.1	P-19	-7.06	-8.73			18
P-20	-7.11	-7.85			8.4	P-20	-7.28	-8.76			17.7
P-22			-8.62	-8.08	7.9	P-22	-7.21	-8.61	-8.97	-8.52	17.6

Table A2. Data of tufa calcite $\delta^{13}\text{C}$ and $\delta^{18}\text{O}$ (‰VPDB), river water $\delta^{18}\text{O}$ (‰VSMOW) and $\delta^{13}\text{C}_{\text{DIC}}$ (‰VPDB), and water T measured during sampling.

Temperature °C	AñamazaRiver		Piedra River								EbrónRiver	
Sites	A-3	A-6	P-14	P-16	P-20	P-8	P-11	P-12	P-18	P-19	E-2	E-8
Cool1999-2000				11.5	11.6		12.5	12.5				
Warm2000				16.3	15.6		12.2	11.6				
Cool2000-2001			12.3	10.4	9.4			11.6				
Warm2001			16.8	16.5	15.8		16.2	11.6				
Cool2001-2002			9.4	9.9	10.4		14.0					
Warm2002			13.3	15.6	12.9		14.4					
Cool2002-2003			14.5	9.4	12.8		10.5					
Warm2003					16.1		15.3	16.1				
Cool2003-2004					14.6		10.6	14.1				
Warm2004			15.3	16.0	16.2		17.4	14.4				
Cool2004-2005			9.0	11.5	10.9		10.9	10.7				
Warm2005			15.8	15.5	15.6		14.3	14.1				
Cool2005-2006			9.9	12.0	11.1		14.2	13.1				
Warm2006			17.7	15.2	13.4		14.3	16.3				
Cool 2006-2007			11.1	16.1	10.8		13.1	13.7				
Warm2007			15.8	19.5	14.5		15.1	15.8			14.2	14.1
Cool2007-2008		8.6	10.6	14.0	10.5		11.3	10.0			16.1	14.5
Warm2008	13.7	14.2	15.3	19.0	16.0		17.8	16.2			12.4	16.4
Cool2008-2009	10.7	9.0	10.8	13.8	10.2		11.1	14.3				12.3
Warm2009	16.7	12.9	15.9	19.5	15.3		15.3	14.7			13.6	16.1
Cool 09-10	9.6	8.1	13.1	12.6	13.0	14.8	14.0	10.8		11.9	11.7	13.4
Warm2010			18.0	15.2	16.8	17.5	17.4	16.9	14.5	13.5		
Cool2010-2011			14.5	11.1	12.5	13.4	13.2	10.8	10.1	14.1		
Warm2011			17.0	16.0	16.5	15.7	15.7	15.0	17.9	16.2		
Cool2011-2012			12.3	10.6	12.0	13.3	13.6	11.2	10.9	11.2		

Warm2012		16.2	14.9	16.6	17.2	17.1	13.0	13.1	16.4
----------	--	------	------	------	------	------	------	------	------

Table A3. Calculated water temperatures from tufa calcite $\delta^{18}\text{O}$ in the three studied rivers

Highlights

- Recent tufa $\delta^{18}\text{O}$ reveal seasonal and decadal climate changes in NE Iberia
- $\delta^{18}\text{O}$ calcite-derived Tw fit regional and local air temperature trends through time
- Calculated Tw can be biased by discharge and rainfall isotopic composition changes
- $\delta^{13}\text{C}$ calcite reflects both exceptional discharge events and in-aquifer recharge
- Together, this is relevant to climate inferences from isotopes in carbonate records